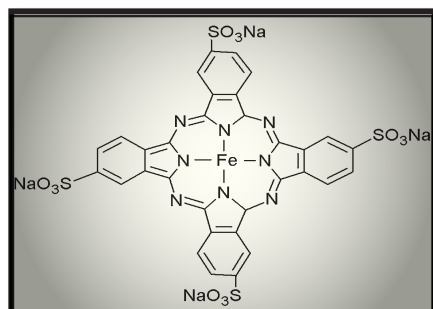
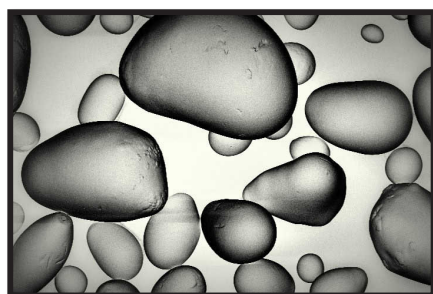
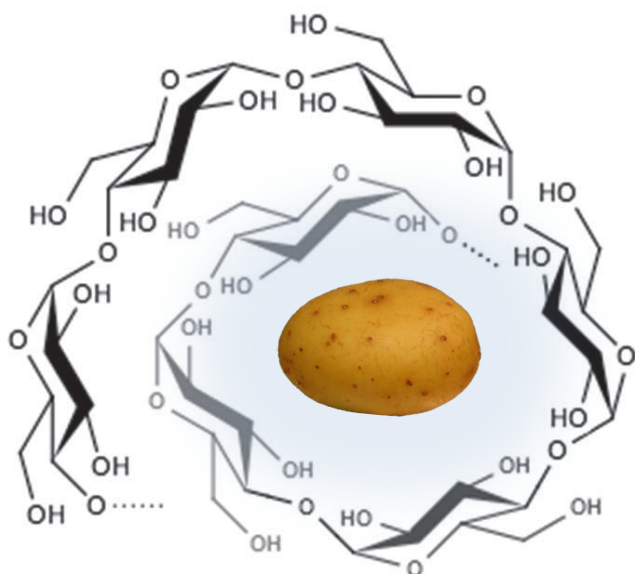


Pasi A. Tolvanen

Development of an Environmentally Friendly Method of Starch Oxidation by Hydrogen Peroxide and a Complex Water-soluble Iron Catalyst





Pasi A. Tolvanen (born 1979)

Masters degree in Åbo Akademi 2006

PhD dissertation defence in Åbo Akademi 2013

Åbo Akademi University Press
Tavastgatan 13, FI-20500 Åbo, Finland
Tel. +358 (0)2 215 3478
E-mail: forlaget@abo.fi

Sales and distribution:
Åbo Akademi University Library
Domkyrkogatan 2–4, FI-20500 Åbo, Finland
Tel. +358 (0)2 -215 4190
E-mail: publikationer@abo.fi

**Development of an Environmentally
Friendly Method of Starch Oxidation by Hydrogen Peroxide
and a Complex Water-soluble Iron Catalyst**

Pasi A. Tolvanen



Laboratory of Industrial Chemistry and Reaction Engineering
Process Chemistry Centre
Department of Chemical Engineering
Åbo Akademi University
Åbo 2013

Supervised by

Academy Professor Tapio Salmi
Laboratory of Industrial Chemistry and Reaction Engineering
Process Chemistry Centre
Department of Chemical Engineering
Åbo Akademi University
Finland

and

Professor Dmitry Yu. Murzin
Laboratory of Industrial Chemistry and Reaction Engineering
Process Chemistry Centre
Department of Chemical Engineering
Åbo Akademi University
Finland

Reviewers

Dr Esko Tirronen
Kemira Oyj
Finland

and

Opponent

Docent Dr Fredrik Sandelin
FT-Engineering
Finland

ISBN 978-952-12-2834-6

Painosalama Oy – Turku, Finland 2013

PREFACE

The present work was carried out at the laboratory of industrial Chemistry and Reaction Engineering, Department of Chemical Engineering at Åbo Akademi University between January 2007 and December 2012.

The project was carried out in cooperation with Institut de recherches sur la catalyse et l'environnement de Lyon, CNRS, France. The financial support from Raison tutkimussäätiö and Stiftelsen för Åbo Akademi is gratefully acknowledged.

I would first of all express my deepest gratitude to my supervisors, Academy Professor Tapio Salmi and Professor Dmitry Yu. Murzin, and docent Dr. Päivi Mäki-Arvela for their endless encouragement and guidance to find the driving inspiration during these exciting years. Without your help this work would not have been possible! Moreover, I appreciate the effort you gave me to this work, as well as to the other research activities we were involved in during these years, which all together have shaped my academic skills to the current level. I am also thankful for the opportunity of being part of organizing committees and as photographer in various conferences in the past and hopefully in the future as well.

A special acknowledgment goes to our laboratory manager Dr. Kari Eränen who has contributed a lot of nerves for the reactor systems developed. Additional credits are given to Dr. Alexander Sorokin for his contribution regarding the catalyst and taught me the analysis procedures during my stay at Lyon. I am also grateful of the help

given by Jarl Hemming and Linus Silvander regarding the analysis methodologies, and the effort given by all co-authors involved.

To all colleagues and friends at the laboratory, present and past – Thank you for your support and encouragement, and for making this laboratory as a second living room, or, sometimes, even as an amusement park – counting the unforgettable conference trips (Malta, Montreal...), the summer schools, even winter schools (Switzerland), summer seminars to Mariehamn, boat trips to Sweden, snowboarding, tennis, table tennis, bowling, pool, Texas hold 'em tournaments, go-karting, just to mention a few – these memories are unforgettable and that is what makes our laboratory elite.

Last but not least, I would like to express my deepest appreciations to my parents, my brother, and lovely Maarit, who have pushed me this far and further, and have not once lacked faith in my chosen path to the world of academia.

ABSTRACT

Pasi A. Tolvanen

Development of an Environmentally Friendly Method of Starch Oxidation by Hydrogen Peroxide and a Complex Water-soluble Iron Catalyst.

Doctoral Thesis, Industrial Chemistry and Reaction Engineering,
Process Chemistry Centre, Department of Chemical Engineering,
Åbo Akademi University, 2013.

Keywords:

starch, oxidation, hydrogen peroxide, FePcS, catalysis, kinetics, ultrasound

Oxidized starch is a key component in the paper industry, where it is used as both surfacing sizer and filler. Large quantities are annually used for this purpose; however, the methods for the oxidation are not environmentally friendly. In our research, we have studied the possibility to replace the harmful oxidation agents, such as hypochlorite or iodates and transition metal catalysts, with a more environmentally friendly oxidant, hydrogen peroxide (H_2O_2), and a special metal complex catalyst (FePcS), of which only a small amount is needed. The work comprised batch and semi-batch studies by H_2O_2 , ultrasound studies of starch particles, determination of low-molecular by-products and determination of the decomposition kinetics of H_2O_2 in the presence of starch and the catalyst. This resulted in a waste-free oxidation method, which only produces water and oxygen as side products.

The starch oxidation was studied in both semi-batch and batch modes in respect to the oxidant (H_2O_2) addition. The semi-batch mode proved to yield a sufficient degree of substitution (COOH groups) for industrial purposes. Treatment of starch granules by ultrasound was found to improve the reactivity of starch. The kinetic results were found out to have a rather complex pattern – several oxidation phases were observed, apparently due to the fact that the oxidation reaction in the beginning only took place on the surface, whereas after a prolonged reaction time, partial degradation of the solid starch granules allowed further reaction in the interior parts. Batch-mode experiments enabled a more detailed study of the mechanisms of starch in the presence of H_2O_2 and the catalyst, but yielded less oxidized starch due to rapid decomposition of H_2O_2 due to its high concentrations. The effect of the solid-liquid (S/L) ratio in the reaction system was studied in batch experiments. These studies revealed that the presence of the catalyst and the starch enhance the H_2O_2 decomposition.

REFERAT

Pasi A. Tolvanen

Miljövänlig katalytisk oxidering av stärkelse med väteperoxid

Doktorsavhandling, Laboratoriet för teknisk kemi och reaktionsteknik,
Processkemiska centret, Institutionen för kemiteknik, Åbo Akademi, 2013.

Nyckelord:

stärkelse, oxidation, väteperoxid, FePcS, katalys, kinetik, ultraljud

Oxiderad stärkelse är en nyckelkomponent inom pappersindustrin, där denna används främst i samband med pappersbetrykningen genom att bidra som bindemedel i pappersmassan samt som fyllmedel vid betrykningsskedet. Årligen används stora mängder stärkelse inom pappersindustrin, men de nuvarande oxidationsmetoderna är inte miljövänliga. I detta arbete har det studerats möjligheten att istället för de kemikalier vilka används idag (såsom hypoklorit eller jodinhållande oxidanter, samt övergångsmetaller som katalysatorer), utveckla en miljövänligare process, där väteperoxid (H_2O_2) samt en speciell metallkomplex (FePcS) utnyttjas, vilket resulterar i en avfallsfri process där endast syre och vatten bildas som biprodukter.

Detta arbete omfattar satsvisa samt halvkontinuerliga reaktionsstudier av stärkelseoxidering med hjälp av väteperoxid, studier av inverkan av ultraljud på

stärkelsepartiklar, bestämning av lågmolekylära biprodukter samt bestämning av väteperoxidens sönderfallningskinetik i närvaro av stärkelse och katalysator.

Både satsvis och halvkontinuerlig process studerades med avseende på oxidationsmedlets (H_2O_2) tillsats. Den halvkontinuerliga metoden gav en bra substitutionsgrad av karboxylgrupper (COOH). Användning av ultraljud konstaterades förbättra stärkelsens reaktivitet väsentligt. Det observerades att både karbonyl- samt karboxylgruppernas bildning hade ett tämligen komplicerat mönster, innehållande flera oxidationsfaser. Detta beror möjligen på det faktum att oxidationsreaktionen i början endast sker på stärkelsegranulens yta, varefter oxidation även inuti granulen efter en fördröjd reaktionstid möjliggörs, då stärkelsegranulerna partiellt degraderas. Satsvisa experiment tillgav värdefull information angående mekanismerna bakom väteperoxidens sönderfall i närvaro av katalysator och stärkelse, men gav klart lägre substitutionsgrad av karboxylgrupper, då väteperoxiden oundvikligt snabbt sönderföll på grund av dens höga begynnelsekoncentration. Effekten av fast-vätskefasförhållandet (S/L) i reaktionssystemet studerades med hjälp av satsvisa experiment. Dessa studier påvisade att närvaro av katalysator samt stärkelse försnabbade väteperoxidens sönderfall.

TABLE OF CONTENTS

PREFACE.....	i
ABSTRACT.....	iii
REFERAT	v
TABLE OF CONTENTS	vii
1. INTRODUCTION.....	1
1.1 The polysaccharide Starch	1
1.2 Starch in the industry	6
1.3 Overview of starch oxidation	10
1.4 Hydrogen peroxide as an environmental friendly oxidant in the industry.....	13
1.5 Starch oxidation by hydrogen peroxide	14
1.6 Aim and scope of the research	19
2. MATERIALS AND METHODS - EXPERIMENTAL SECTION	21
2.1. Raw materials.....	21
2.2 Standard starch oxidation procedure.....	23
2.3. Procedure for S/L-ratio and catalyst concentration experiments	26
2.4. Product analysis	28
2.5. Starch treatment with ultrasound	29
2.6. Surface area measurements	31
3. KINETICS, MECHANISM AND MODELING	33
3.1 Reactions of hydrogen peroxide.....	33
3.2 Results obtained from H ₂ O ₂ decomposition	34
3.3 Kinetic results of semibatch experiments	35

3.4. Granular structures and residual iron content by SEM-EDXA – semibatch experiments	43
3.5 Kinetic results and discussion of batch mode experiments.....	45
3.5.1 Kinetic results.....	46
3.5.2 Low molecular weight compounds	48
3.5.3 Catalyst solution feed (Table 3.3, entry 4).....	48
3.5.4 Ultrasound-pretreated starch	50
3.5.5 Reaction mechanism	53
3.5.6 H ₂ O ₂ decomposition studies.....	54
3.5.7 Modeling of H ₂ O ₂ decomposition.....	55
3.6 Effect of the catalyst concentration and the solid-to-liquid ratio.....	62
3.7 Effect of the starch origin.....	67
3.8 Effect of amylopectin and amylose contents	70
3.9 Formation of carboxyl groups from S/L experiments.....	71
3.10 Fragmentation of iron from the catalyst complex	72
3.11 Analysis of COOH and C=O concentrations of the solid starch by HPLC	73
3.12 Analysis of low molecular weight compounds by GC-MS	74
3.13 Analysis performed with Q-TOF	76
3.14 Additional SEM analyses of solid starch samples	77
3.15 Product coloration	88
4. CONCLUSIONS	91
NOTATION.....	93
REFERENCES	95

1. INTRODUCTION

Starch is a natural polysaccharide, produced (as an energy storage) by all green plants found in nature. It is a part of our daily energy source in the form of food. Starch can also be industrially modified i.e. by oxidation in order to obtain special properties. Oxidized starch is an important component in the manufacturing of paper, more precisely in the coating process. The commonly used method for oxidizing starch is by using harmful stoichiometric oxidants such as chlorites or periodates, combined with heavy metal sulphates as catalysts. Environmental concerns and regulations have increased lately in the public as well as political world, and hence the industry strives for more clean processes. Therefore in this work it will be presented that for industrial starch oxidation, it is possible to reduce the formation of inorganic by-products by replacing the harmful oxidants and catalysts with environmentally friendly ones.

1.1 The polysaccharide Starch

Principally all green plants such as potato, corn, wheat, rice, cassava consist of a macromolecule called starch. It is the nature's own type of energy reserve. In the food processing industry, pasted starch is used as a thickener.

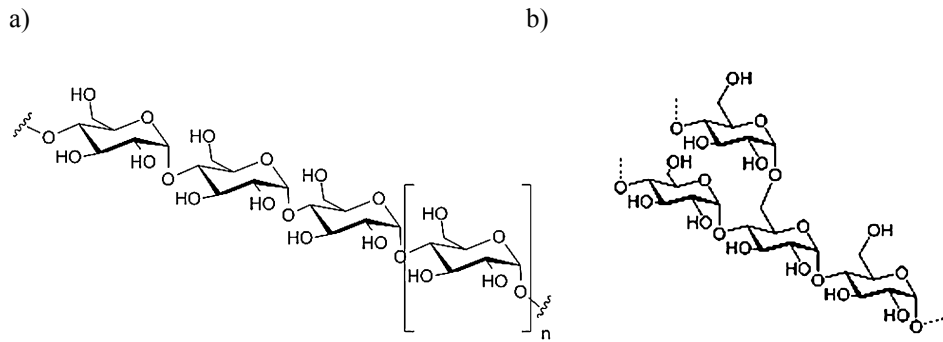


Figure 1.1. Starch consists of **a)** the linear molecule amylose and **b)** branched molecule amylopectin in different proportions, depending on the origin. The anhydroglucose unit (AGU) is given with brackets [].

Raw starch granules are compact and therefore not suited to digest as such. In order to increase its digestibility, the raw starch needs to be cooked to become water-soluble and edible. When starch is heated in hot water it is transformed – the branched amylopectin molecule (Figure 1.1) swells and causes the crystalline structures to melt and break free, and eventually allows the amylose to leak into the surrounding water, forming a paste (gelatinization). During cooling or prolonged storage, the starch paste thickens due to a phenomenon called retrogradation. For potato starch the gelatinization occurs typically around 58-62 °C.

When separated from the plant, the starch is in a solid, usually round or oval shaped granular form and the size of the granules range from a few μm for rice, up to 100 μm for potato starch granules, but the dispersion is broad. The granules consist mainly of two different types of polymers named amylose and amylopectin (Figure 1.1). Both components contain polymer chains of glucose units, but the chains are linked differently. Amylose is predominantly linear and the glucose units are linked together

with linear $\alpha(1\rightarrow4)$ bonds, whereas amylopectin is more branched with $\alpha(1\rightarrow6)$ glycosidic bonds, see Figure 1.1.

The ratio of the amylose to amylopectin as well as the chain length distribution, granular size and lipid content varies in starches from different sources, e.g. unmodified potato starch contains approx. 20 % amylose and 80 % amylopectin [1]. The glucose units have three hydroxyl groups which are available for reaction. Additionally to amylose and amylopectin, starch also consists of a small amount of other compounds such as lipids, proteins and phosphates. When observing the structure of a starch granule on a larger than atomic scale, it becomes more complex. Even though the exact structures variate from one starch origin to another, generalities can be drawn. For instance, the proportions of amylose and amylopectin differ much, however 10-30 % tend to be amylose and the rest is amylopectin. At the lowest level of structure, the amylose and amylopectin chains form clusters (0.1-1 nm), which are joined together forming lamellae (10 nm), and blocklets (20-250 nm), which in turn build up the so called growth rings, which alternate by amorphous and crystalline structure from center (hilum) until the granule periphery (1000 nm), see Figure 1.2.

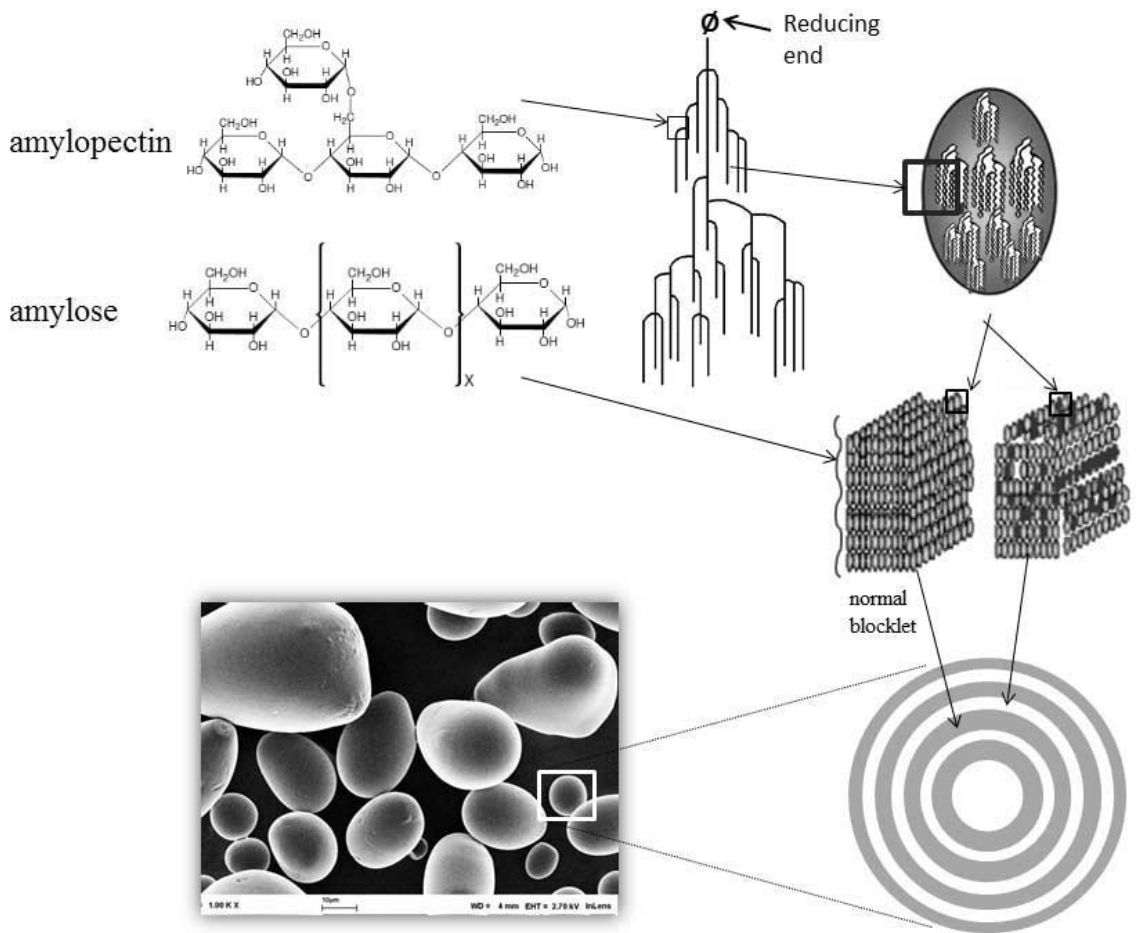


Figure 1.2. The structure of starch from atomic to granular level starting from amylose and amylopectin to complete granules.

The granule size and shape differs depending on the botanical source. Some key properties of some of the most common commercial starch granules are listed in Table 1.1.

Table 1.1. Average values for native starch granule properties from different botanical sources [2].

Granule properties	Potato	Maize	Wheat	Tapioca	Waxy maize
Type and shape	tuber, oval, spherical	cereal, round, polygonal	cereal, round, lenticular	root, truncated, round, oval	cereal, round, polygonal
diameter, range (μm)	5-100	2-30	1-45	4-35	2-30
Diameter, number average	27	10	8	15	10
Diameter, weight average (μm)	40	15	25	25	15
Number of granules per g of starch ($\times 10^6$)	60	1300	2600	500	1300
Av. number of starch molecules in one granule ($\times 10^{12}$)	50	10	5	4	0.01
Specific area (m^2 / kg)	100	300	500	200	300
Gelatination temperature	60-75	75-80	80-85	65-70	65-70
amylose/amylopectin %	21/79	28/72	28/72	17/83	0/100
Average degree of polymerization of starch molecules	14000	3000	3000	18000	2000000

1.2 Starch in the industry

Starch is an important and interesting biopolymer for the industries nowadays, due to its large availability and low cost. Thickening agents, stabilizers, emulsifiers, fuel ethanol, as well as bio-plastics, can be produced from native starch. In the paper industry, starch is heavily deployed as a sizing agent as it improves the mechanical and film-forming properties of paper, paper board and textiles by binding together the components of paper web (fibers, pigments, fillers).

Starch production has recently been growing worldwide. The starch processing industry has diversified its products from a basic product (native starch) with limited uses to a large range of valuable ingredients for food and non-food sectors [3]. Starch is relatively cheap and abundant and thus recent research has been focused on modifying or transforming it into a wide range of products, such as bio plastics, ethanol fuel, fine chemicals as well as vitamins, adhesives and surfactants.

Starch as such is not suitable for the industry and must thus be chemically or mechanically modified to achieve the properties required for the particular application. Starch is generally modified in such way that the solid granular form is maintained and the aqueous reactant media is filtered away. The most typical modifications of starch include hydrolysis by enzymes or acid, oxidation, esterification, and etherification [1]. It is possible to tailor the physical properties of the starches such as viscosity, lubricity, and freeze stability to meet the specific requirements of the intended application.

Starch derivatives are widely used in a broad range of industries, for instance, in the food industry as thickeners and gelling agents, in paper making as wet-end additives and surface improvement as well as adhesives, and in mining industry as completion fluids. Starch is also deployed in pharmacology products i.e. tableting and cosmetic formulations, in plastics for enhancing degradability. Starches rich in amylose form rigid, opaque gels on cooling (due to retrogradation), which on storage lose the water molecule (syneresis), whereas starches rich in amylopectin (waxy-type) form soft gels. The major starch end-use sectors by starch products are listed in Table 1.2.

Table 1.2. Major starch end-use sectors by starch product [3].

Native starches	
Potato native starch	
maize native starch	Paper and cardboard industry; Food industry
Wheat native starch	
Barley native starch	Paper industry or potable alcohol production
Hydrolysed starches- Sweeteners	
	Maltodextrins:
	- food preparation (bulking agent)
	- Pharmaceutical (excipient)
	- Ingredient in ice cream industry
Hydrolyzed starch	
	Glucose syrup:
	- Dextrose Equivalent of between 40 and 60: food industry
<i>maltodextrins, glucose</i>	
<i>syrups, hydrolysates</i>	- Beverage and confectionary industry
	Hydrolysates:
	- Used directly as substrates for producing fermentation products, such as citric acid, lysine or ethanol or glutamic acid
	- Processed into other major starch derivatives such as isoglucose, fructose syrup, etc.
Modified starches: types of modifications	
Substituted starches	Textiles (warp sizing: lubrication and abrasion resistance, printing)
<i>Starch esters, ethers,</i>	Paper (Internal sizing, coating and surface sizing: strength, stiffness and ink resistance)
<i>cross-linked starch)</i>	Water treatment (flocculation)
	Oil industry (fluid loss reducer)
Defraded/ Converted starches	Dextrins: Adhesives (gummed paper, bag adhesives, labelling); Textiles (textile fabric finishing, printing);
	Acid-modified starches: Food industry (sweets)
<i>Roast dextrin, oxidized</i>	Oxidised starches: Paper industry (surface sizing, coating); textile industry (fabric finishing, warp sizing)
<i>starch, thin-boiled starch</i>	Enzymatically converted starch: paper industry and fermentation industry
Cross-linked starches	Food industry (desserts, bakery products, soups, sauces), textile industry (printing)
	adhesives, pharmaceuticals

Source: Agrosynergie elaboration, Chemistry and Technology (3rd Edition), 2007; LMC (2002)

The papermaking industry uses a large amount of starch each year, since it provides functional properties and serves as a process aid. Starch is the highest amount of material used in paper making after water, fibers and fillers. It has been part of both for sizing and coating of paper as long as the printing technique was invented by Gutenberg. It is used in several different steps in the process, the wet end and on the size press. The global paper industry is currently estimated to use 5-6 million tons of starch annually as per year 2012 [4].

In this study, the formation of carboxyl and carbonyl groups has been the primary focus. When carboxylic groups are introduced into the starch, they sterically hinder the associative tendencies. Starch derivatives that have an average of two or more constituent groups per glucose unit are considered to be highly substituted starches, while those having an average of 0.2 or less are considered to have a low degree of substitution (DS). Generally, the degree of substitution (DS) of commercial starches is less than 0.2. Already a low level of substitution gives several benefits such as retarded retrogradation, an increased water binding capacity, or a lowered gelatination temperature [5].

1.3 Overview of starch oxidation

Several different oxidants can be used for starch oxidation such as hypochlorite, bromine, periodate, permanganate ammonium persulphate and hydrogen peroxide (H_2O_2). Hypochlorite is the most common of these in an industrial scale, mainly due to its effectiveness and the absence of a catalyst, although the use of hypochlorite leads to the formation of toxic chlorinated by-products [6]. Fully water soluble wheat starch with high carboxyl content, oxidized in acidic bromate reaction media at room temperature without any catalyst added, has recently been reported [7]. Interestingly, the study discovered that the concentration of carbonyl groups decreased after a prolonged reaction time indicating that the oxidation mechanism follows a consecutive reaction pattern, where firstly, carbonyl groups are formed, which are then in turn oxidized further to carboxyl groups. This mechanism was similar to the one proposed in our previous study, however, with a different oxidant (bromate instead of H_2O_2) and no catalyst [8,9]. According to the mechanism, bromate can carry hydroxyl radical species in a similar way as the catalyst FePcS.

A study, in which the carboxyl group concentration was profiled inside the starch granule, revealed that COOH concentration dropped significantly towards the starch particle centre [10]. The profile was obtained by a method called chemical surface gelatination, where the outermost layers are removed and the oxidized starch is analyzed at different radial locations within the granule. Therefore, by i.e. chemical degradation or by deterioration of the surface by ultrasound treatment, more surface area would become available for oxidation and higher degrees of substitution consequently achieved. To understand this phenomenon in more detail, experiments were performed by alternating the solid-to-liquid ratio in the experiments.

The physicochemical properties of starches which have been oxidized by either sodium hypochlorite or H_2O_2 have been shown to vary significantly, for instance, hypochlorite oxidation favours carboxyl group formation, while H_2O_2 favours carbonyl groups [11]. The study also showed that the product formation was faster in the case of H_2O_2 , and that the peroxide-oxidized starch possessed higher tendency for gelation and gave a firmer gel. Therefore, there is an additional benefit for studying the starch oxidation by H_2O_2 instead of stoichiometric oxidants.

Some previous investigations have shown that potato starch is much more prone to oxidation than, for instance corn, and rice starches under the similar oxidation conditions. This can be due to the loose arrangement of the B-type crystalline structure [12] in the potato starch, which may provide more accessible sites for oxidation [10].

Additionally, the amylopectin-to-amylose ratio has a large influence on the properties of modified starches. Amylose has a linear structure, mainly comprising 20-30 wt.-% of the starch. Due to the linear structure, it is tightly packed, and is more resistant to i.e. digestion than its counterpart amylopectin. It might therefore be possible that it is also more resistant for a chemical transformation. The influence of the amylopectin-to-amylose ratio in the starch oxidation has been studied previously, and it has been shown that in combination of H_2O_2 and a heavy metal catalyst (cupric and ferrous sulfate), moderate oxidation was achieved, although the high-amylopectin starch yielded lower COOH formation compared to high-amylose starch [13], and, in general, the oxidation degrees were lower than in the case of native potato starch oxidized by tungstate (Na_2WO_4) or copper/iron sulphate in combination with H_2O_2 [24].

Moreover, there lies a commercial interest in the potential success of starch oxidation with a high amylopectin content. Genetic experts have recently developed a high-quality amylopectin containing potato, Amflora, which is more suitable for technical purposes, i.e. the properties needed in the paper industry, such as higher gloss of the paper surface and reduced consumption of energy [14]. For many technical applications, such as in the paper, textile and adhesives industries, pure amylopectin is advantageous, however, separating the two starch components is uneconomical. Therefore, it would be beneficial for the industry to use high-quality Amflora starch in order to optimize the industrial processes: it gives paper a higher gloss, and concrete and adhesives can be processed for a longer period of time. This reduces the consumption of energy, and reduces the usage of additives and water [15]. Since Amflora was not yet to date available, a corn starch with high amylopectin content was used instead. Regular potato starch was used in some experiments for comparison of the results.

1.4 Hydrogen peroxide as an environmental friendly oxidant in the industry

Hydrogen peroxide is the simplest peroxide consisting of only two hydrogen and two oxygen atoms, H_2O_2 . It is a clear liquid at room temperature and in pure form it is a bit denser than water, however due to safety reasons it is normally used in diluted form. Pure hydrogen peroxide has a pH of 6.2 and it is considered to be a weak acid.

Hydrogen peroxide is sensitive for decomposition e.g. sunlight or metal impurities.

There exists a general trend in the industries to develop clean and eco-efficient oxidation processes in order to minimize the formation of harmful by-products. In the bulk chemical industry for manufacturing e.g., ethylene oxide, formaldehyde, phthalic anhydride, environmentally unacceptable processes have already been replaced by cleaner catalytic procedures, whereas fine and intermediate chemicals are still widely produced via traditional stoichiometric oxidations which produce waste. Still up to date, organic chemists employ stoichiometric oxidants such as dichromate/sulfuric acid, chromium oxides, permanganates, periodates, osmium oxide, or hazardous chlorine causing high salt freights and heavy metal-containing dumps unable to be recycled, as well as relatively expensive hydroperoxides, alkylperoxides, and peroxy-carbonic acids [1].

1.5 Starch oxidation by hydrogen peroxide

The main reason to chemically treat starch before the commercial use is to split the long glucose chains of the polymer molecules in order to reduce the high viscosity of unmodified starch solutions and thereby increase and maximize the possible starch amounts in technical applications. The reduction of the average chain length can be done – and also in practice is done - by numerous different ways. These include in addition to oxidation also for example acid hydrolysis and enzymatic modification.

Thus, before starch can be used, it has to be modified by e.g. oxidation. Numerous oxidation methods are known, e.g. wet-, semi-dry and dry oxidation as well documented in [16]. Oxidation of starch allows carboxyl and carbonyl groups to be substituted on the polymer backbone, replacing the hydroxyl groups. Oxidized starch having a degree of substitution (DS) of 0.01-0.20 (1-20 substituted units per 100 AGUs) is of commercial interest. Traditionally, oxidation has been performed with heavy-metals (iron, copper, tungsten) as catalysts, and NaOCl (hypochlorite) or N₂O₄ as oxidants, which all produce large quantities of inorganic waste. Oxidation by hypochlorite is one of the oldest method which is still widely used in industry [17]. Hypochlorite is a powerful and mainly used oxidant for oxidation of starch, but if the industry would use hydrogen peroxide instead of hypochlorite, only acceptable reaction products in the slurry are formed, hence making this an attractive choice. It is possible to increase the reaction at an elevated temperature, but this is not possible if starch is oxidized in a different facility, since it must remain in a granular form - a property of no importance when the starch is modified, cooked and used in situ.

When polysaccharides are oxidized, a reaction can take place on several different locations of the anhydroglucose unit. Uronic acids (a class of sugar acids with carboxylic acid groups) are formed when the terminal carbon's (C6) hydroxyl group is oxidized to a carboxyl group, whereas oxidation of the terminal aldehyde groups gives aldonic acids.

Iron sulphate as a catalyst can penetrate to the interior of the starch granule since the molecule is small enough. On the other hand, iron is known to form complexes with starch and thus it remains inside of the granule, resulting in coloration and loss of catalyst efficiency.

Thus, a new environmentally friendly method for starch oxidation was developed, by deploying a novel efficient iron complex FePcS (iron tetrasulfonatophthalocyanine) as a catalyst and hydrogen peroxide as an oxidant [18]. Compared to the efficiency of iron (II) sulphate, 20 times less FePcS (see Figure 2.1) catalyst is needed to achieve the same oxidation degree. Additionally, the oxidized starch product contains practically the same iron content as the native potato starch, whereas prepared with iron salt as a catalyst the oxidized starch had a significant level of residual iron due to complexation, causing an undesirable coloration and loss of the catalyst [18].

The exact reaction paths in starch oxidation are not yet completely understood. Probably the most accepted reaction path is described by Floor [19], Figure 1.3, in which two competing reaction paths take place. The relationship between the formation of carboxyl and carbonyl groups is unclear. It is reported, that hydroxyl groups in starch molecules are first oxidized to carbonyl groups and *then* to carboxyl

groups, which primarily takes place at C-2, C-3, and C-6 [20,21]. This would indicate that the reaction path is consecutive with carbonyl groups as intermediates, which react further to carboxyl groups after prolonged reaction times. On the other hand, parallel reaction paths are, however, also reported. Depending on type of oxidant used, carbonyl groups are selectively formed by oxidation of the hydroxyl groups at the positions C₂ and C₃, whereas with another oxidant, the hydroxyl groups at the position C₆ form carboxyl groups [22].

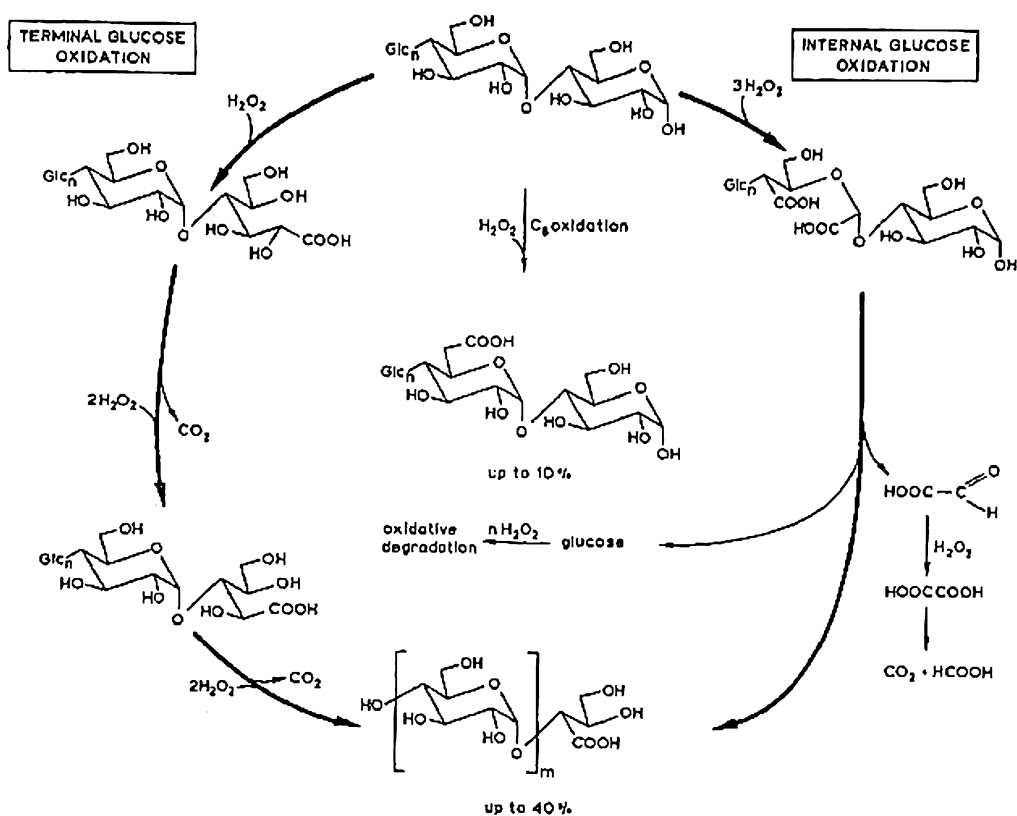


Figure 1.3. The possible reaction paths and formation of low molecular weight products during polysaccharide oxidation by H_2O_2 [19].

The kinetics of starch oxidation reactions has not been previously studied, since most experiments were performed in batch reactors analyzing only the final product [18,19,23]. In some cases, experiments have been performed at different reaction times, and analysis data have been collected from each separate experiment to represent kinetic results of one single experiment [22,24,25]. This procedure is a straightforward but time consuming and expensive approach. Additionally, these methods lack the possibility to monitor changes of the solid to liquid ratios, gas phase analyses, and their dependencies on the oxidant concentration. In the present study the aim was to monitor the progress of the reaction by taking several samples during experiments. This give the possibility to follow the formation of the two product types, carboxyl and carbonyl groups substituted to the backbone of the starch polymer during the reaction, revealing the pathways, which could be either consecutive or parallel. Such investigations of the starch oxidation kinetics using a semibatch reactor may be, however, challenging, since each sample has to contain at least 5-10 grams of solid starch and thus the reactor size must be chosen accordingly.

To preserve the granular form of the starch, the reaction temperature cannot exceed the gelatinization temperature, which is specific to the origin of the starch. H_2O_2 decomposition, which can take place during starch oxidation and is highly exothermic (98.2 kJ/mole), and has to be taken into account to avoid gelatinization.

The rate of H_2O_2 decomposition is dependent on the temperature and concentration of the peroxide, as well as the pH and the presence of impurities and stabilizers. The decomposition occurs more rapidly under alkaline conditions, indicating that acid is often added as a stabilizer. In the presence of certain catalysts, such as Fe^{2+} or Ti^{3+} ,

the hydrogen peroxide decomposition may proceed via a different path, i.e. with free radicals such as HO· (hydroxyl) and HOO· being formed [26].

The catalyst which is in the focus of our research is iron tetrasulfophthalocyanine (FePcS), an iron metal complex which has shown to be an active, selective and stable catalyst combined with an environmentally friendly oxidant H₂O₂. In contrast to the porphyrin complexes, phthalocyanine counterparts are cheap and readily accessible on an industrial scale: their worldwide production is about 80 000 t/year, making them very attractive as potential industrial catalysts. When H₂O₂ decomposes naturally, water and oxygen is formed. However, in the right conditions and with the aid of a suitable catalyst, it is possible to produce hydroxyl radicals and steer them to the substrate, resulting in the wanted reaction. In the presence of iron tetrasulfophthalocyanine, H₂O₂ form nucleophilic species like PcSFe^{III}-OOH and electrophilic species like PcFe^{IV}=O or PcFe^V=O. these species are capable of degrading compounds that are resistant to e.g. H₂O₂ oxidation [27].

1.6 Aim and scope of the research

Traditional methods of starch oxidation with stoichiometric oxidants produce large amounts of inorganic waste. This work has developed further an environmentally friendly option for starch oxidation, using an iron tetrasulfophthalocyanine complex (FePcS) as a catalyst and as an oxidant H_2O_2 , which forms only water as by-product. The important advantages of FePcS catalyst are (i) only a small amount of catalyst is needed for efficient oxidation; (ii) its good solubility in water permitting ready reaction with heterogeneous starch substrate in aqueous medium and (iii) the absence of complexation products with the oxidized starch. Oxidation of starch with hydrogen peroxide has been reported to work [8,9,18], but the rigorous treatment of the reaction kinetics is absent as well as the reactor technology (batch contra semibatch operation). The FePcS catalyst may not be able to penetrate into the granules which would lead to catalytic reactions only on the surface of the granules. Therefore it was studied whether ultrasonic pre-treatment of starch could create cavities on the starch granule surface allowing reaction to take place inside the granules, thus leading to a higher degree of substitution. A lot of efforts have also been put in the identification of low molecular weight products and reactions behind them. The present work evaluates the effect of temperature, hydrogen peroxide concentration, pH, and solid-to-liquid ratio on the oxidation of starch. Furthermore, the depolymerization of the starch to soluble starch, the formation of low molecular compounds, and the actual concentration of hydrogen peroxide were investigated. The oxidation reaction has been studied in this work to develop mathematical models based on physico-chemical understanding of solid (starch) reactions with liquids (H_2O_2) as well as to create a basic understanding of the reaction mechanism.

2. MATERIALS AND METHODS - EXPERIMENTAL SECTION

2.1. Raw materials

Native potato starch, regular corn starch, high amylose corn starch for oxidation experiments and dialdehyde starch (used for HPLC analysis) were purchased from Sigma–Aldrich. Hydrogen peroxide (30 wt.%, Merck), was utilized as an oxidant, and the pH was maintained at desired level by pH stat device by using 0.2 - 2 M NaOH. Water soluble iron tetrasulfophthalocyanine was prepared by a modified Weber-Busch procedure as described previously [28, 29] The molecular structure of the catalyst is illustrated in Figure 2.1a. The catalyst's distinctive blue color in metallic form as well as in water solution is shown in Figures 2.1b-c. The carboxyl group content was determined by titration with 0.025 M NaOH according to a modified version of Smith's method [30]. The carbonyl group content was determined by titration with hydroxyl amine. The hydrogen peroxide content in the samples was determined by iodometric titration (KI, Sigma-Aldrich, 2 M H₂SO₄ for acidification, 0.05 M Na₂S₂O₃ solution).

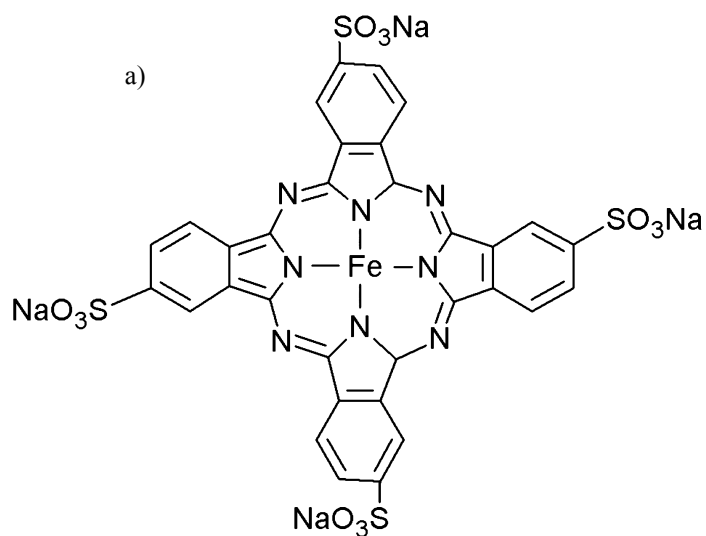


Figure 2.1. a) The chemical structure of the FePcS catalyst, b) the catalyst FePcS in powder form, c) as little as 1.0 mg of the FePcS catalyst dissolved in 10 ml water gives a dark blue solution.

2.2 Standard starch oxidation procedure

The semibatch and batch mode experiments were performed in a 1000 ml glass reactor (Figures 2.2-2.3) according to procedures described in ref. [8, 9]. Typically, 260 g of starch was suspended in deionized water at room temperature, and added into the reactor, after which it was heated up to the desired temperature (semibatch 55 °C, batch 52 °C) and the pH was adjusted manually to the desired level by adding 2 M NaOH solution. In the first study all H₂O₂ was added continuously [8], whereas in the second study [9] all H₂O₂ (70-75 g, 30 wt.%) was added instantaneously, and the initial concentration (c_0) was checked and readjusted prior to the catalyst addition (i.e. c_0 was the same in all experiments). The catalyst was added by dissolving it in 10 ml of water and poured into the reactor. In some of the experiments, the possible deactivation (or loss) of catalyst was studied by dissolving the total amount of catalyst in a larger quantity of water, and the catalyst solution was fed to the reactor at a constant rate (10 mg cat/h) during the experiment (whereas H₂O₂ was added initially).

In the case of batchmode experiment, the temperature (52 °C) was chosen due to pre-cautiousness, since it was observed that when adding all H₂O₂ at once, a slight temperature increase occurred after adding the catalyst and a slight drop of the concentration of H₂O₂ was noticed. Since the potato starch gelatinizes approximately at temperatures exceeding 57 °C, a reaction temperature of 52 °C seemed to be a good choice and the results achieved were still comparable with those achieved in previous semi-bath experiments. The semibatch mode experiments allowed a higher reaction temperature (55-58 °C), since the H₂O₂ concentration remained low and therefore the risk for an exothermic “run-away” was minimal.

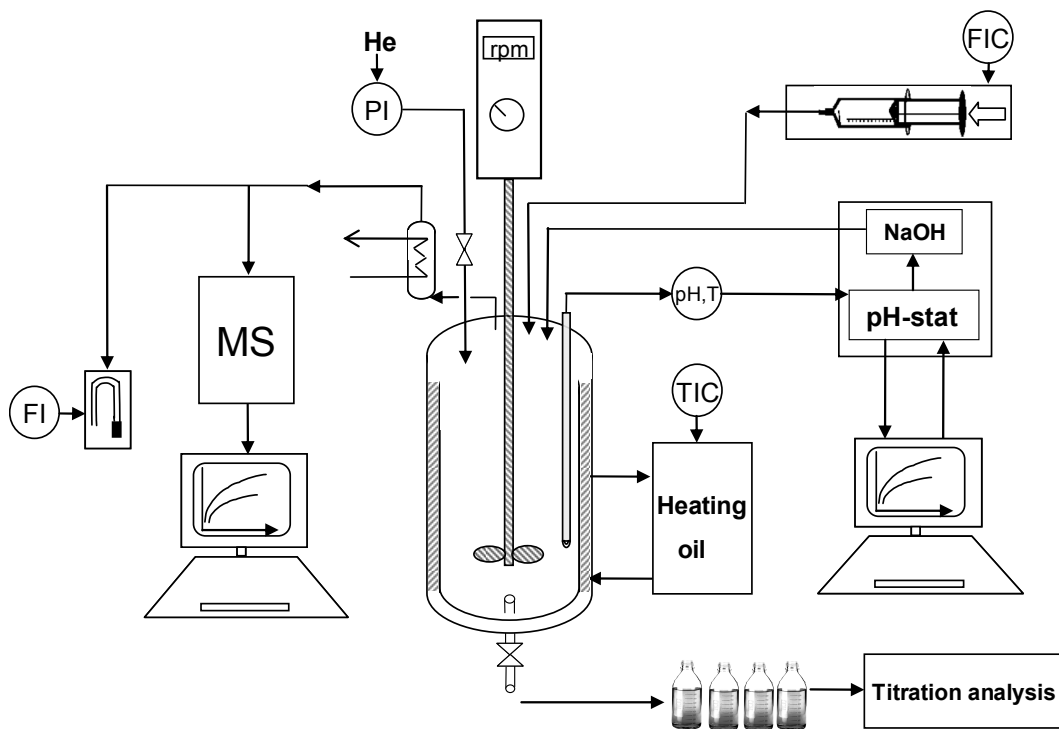


Figure 2.2. Schematic figure of reactor setup.



Figure 2.3. Photo of the reactor.

In order to reveal the decomposition process of H_2O_2 , which proceeds in parallel with the starch oxidation, some experiments with the catalyst and H_2O_2 only were performed at three different temperatures. First, 500 ml of water was added into the reactor and heated up to the desired temperature (52-72 °C), thereafter the pH was adjusted to 8.4 and 35-40 g of 30 wt.% H_2O_2 was added. The initial concentration was checked and adjusted, before the addition of 70 mg catalyst dissolved in 20 ml water.

2.3. Procedure for S/L-ratio and catalyst concentration experiments

Semibatch and batch experiments were performed in a 250 ml glass reactor with recirculating water inside the reactor jacket (Figure 1) to maintain the temperature at desired level. The mixture was agitated with a glass stirrer (700 rpm). A specific amount of starch (0-55.71 g) was suspended in 120 ml deionized water at room temperature and added into the reactor, after which the solution was heated up to the desired temperature and the pH was adjusted manually to the desired level (7-10) by addition of 2 M NaOH. All H_2O_2 was added instantaneously, and the initial concentration of H_2O_2 (c_0) was determined by titration prior to the catalyst addition. The catalyst was added by dissolving it in 10 ml of water and poured into the reactor.

The amount of starch varied from 1.55 – 55.71 g, the water amount was fixed to 120 ml and 10.0 g of 30 wt.-% of H_2O_2 was added in the beginning of reaction (batch-mode). The exact initial H_2O_2 concentration was determined by iodometric titration prior the catalyst addition. The temperature was maintained at 52 °C with circulating heating oil. 2 M NaOH was fed with a pH-stat device to keep the pH at desired level

(usually 8.4). The reactor system was also equipped with a mass spectrometer for possible measurements of gas phase products [8], and a precision pump for feeding H₂O₂ continuously to the reactor if needed (Figure 2.2).

Since a smaller reactor was used than in the studies focusing on the batch or semibatch reactions [8, 9], less starch was subsequently needed. The solid-to-liquid ratio (S/L) 1.0 corresponds to 37 g of starch in 120 ml of water, since the same ratio was used in earlier experiments. Thus, 37.14 g starch is 1/7 of the quantity used in [8]. The S/L ratio was varied in the range of 1/24 to 3/2, and the catalyst amount was 0, 10, 20 or 40 mg. Amount of 20 mg corresponds to the same amount which was used in earlier experiments. The experimental matrix is shown in Table 2.1.

Table 2.1. Experimental matrix for solid-to-liquid ratio experiments. S/L = solid-to-liquid ratio.

	starch,g	no catalyst	10 mg	20 mg	40 mg
S/L 3/2	55.71	x	x y	x	x y
S/L 1.0	37.14		x	x	x
S/L 2/3	24.76	x	x y	x	x y
S/L 1/3	12.38		y	y	x y
S/L 1/6	6.19		y		x y
S/L 1/12	3.10				x
S/L 1/24	1.55				x
	no starch	x	x	x	x y

x=corn starch y= potato starch

2.4. Product analysis

During the experiments, samples were collected at certain time intervals and the H_2O_2 concentration was immediately analyzed by iodometric titration. The experiments were continued until the H_2O_2 concentration was close to zero (or alternatively until the concentration did not decrease significantly).

The low molecular weight compounds were analyzed by GC-MS; 2 ml of the aqueous phase was withdrawn from the sample and the organic phase was extracted by ethyl acetate after addition of sulphuric acid. Finally, the sample was brought to pH 5.5-6.0 with HCl and stored at 4 °C prior filtration to dry product. By measuring the final weight of all dried, solid starch that was left after the experiment, as well as the dried withdrawn samples, the total mass balance was checked. The ratio of the residual solid starch weight and the initial starch weight (the recovered solid starch) was defined as the yield. The loss of solid starch was due to the depolymerization of the starch to aqueous products (e.g. sugar acids and formic acid).

The solid air-dried starch was analyzed for the carboxyl (-COOH) groups by the Smith titration method: 2.5 g air dried starch (-COONa) was stirred in 0.1 M HCl-ethanol-water (2:1) mixture for 30 minutes, thereafter it was filtered and washed off from chlorine. The starch (now in the -COOH form) was gelatinized in an oil bath for 30 minutes and then cooled to 60 °C followed by titration with 0.25 M NaOH to pH 8.30, to determine the amount of COOH groups.

In order to analyze the low molecular weight compounds from the reaction samples, 2 ml of the aqueous phase was acidified with sulphuric acid and the low molecular weight compounds were extracted twice with the aid of ethyl acetate. The extractive was analyzed with GC-MS to identify the species, and thereafter with GC to obtain the quantitative values of the concentrations. Betulinol was used as an internal standard. The column was HP-1 column with FID detector type (length 25 m, 0.199 mm inner diameter, 0.11 mm film thickness). Temperature program used was 50 °C (1 min), 50°C → 170 °C (6 °C/min).

2.5. Starch treatment with ultrasound

Starch was pretreated with ultrasound for 24 h in order to study the sonification effect on the starch granules, i.e. structural changes, and differences in the oxidation kinetics. 280 g of native starch was mixed with 400 g deionized water and placed in special home-made bath type ultrasonic equipment, consisting of a container surrounded by six ultrasound transmitters and a mechanical stirrer, see Figures 2.4-2.5. Ultrasound (6 x 50 W) with the frequency 20 kHz was applied in a cycle of 1 min on/off interval for 24 h. No external heating was applied, but the temperature increased to 36 °C due to the ultrasonic effect. The increase in the temperature to 36 °C, however, is not relevant since starch is gelatinized at much higher temperature, 57-58 °C. The reason for choosing 24 h was that the batch experiments performed at pH 8.4 usually lasted around 24 h before all H₂O₂ had been consumed. The starch was rinsed with water and dried thereafter, and weighed after 48 h of drying on paper sheets under atmospheric conditions and a part of this starch was further analyzed by

SEM. A confirmation test with an aluminium foil was successfully performed to ensure that cavitation bubbles are formed in the ultrasound system, see Figure 2.4. The actual power dissipated in the system in principle can be lower than the nominal power, however, this was not measured. Ultrasound has previously been shown to enhance the selective leaching of sphalerite by enhancing local mass transfer. A nominal input power of 120 - 180 W was shown to be comparable to increasing mechanical agitation from 350 rpm to 500 rpm, with a conventional pitch-blade turbine impeller [31,32].

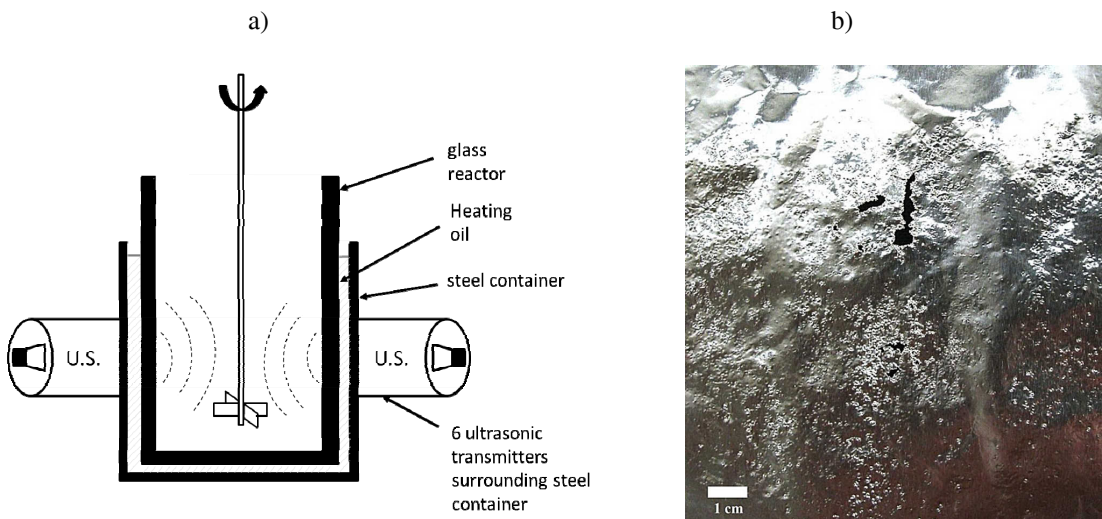


Figure 2.4 a) Schematic of the ultrasonic device applied in experiments, and b) ruptures and large holes in the aluminium foil used in the aluminium foil test confirmed the formation of cavities (the foil was exposed for 1 minute in the glass reactor which was filled with water).



Figure 2.5. A photograph of the ultrasound device into which the reactor was placed when performing sonofication experiments.

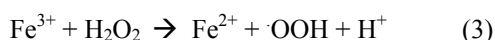
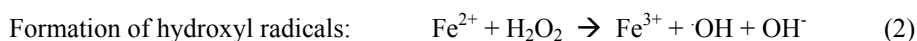
2.6. Surface area measurements

Nitrogen adsorption with a sorptometer (Sorptomatic 1900, Carlo Erba) was used for surface area measurements of native as well as oxidized starch samples. The solid starch sample was washed with ethanol and dried in an exsiccator for 24 h prior to the analysis, to remove water entrapped in the granules.

3. KINETICS, MECHANISM AND MODELING

3.1 Reactions of hydrogen peroxide

Reactions of hydrogen peroxide are well known. H_2O_2 spontaneously decomposes to oxygen and water (eq. 1) and the rate of decomposition is dependent on the temperature, concentration and impurities. However, it can also, especially in the presence of a catalyst, form hydroxyl radicals. The peroxide is broken down into a hydroxide ion and a hydroxyl free radical (eq. 2 and 3). Moreover, radical interactions can lead to recombination of hydrogen peroxide (eq. 4).



The reaction mechanisms of hydrogen peroxide with starch are very complex and may change when changing the reaction conditions. Generally, though, the reaction follows a mechanism similar to the one listed below, in which the formed hydroxyl

radical formed oxidizes an alcohol group on the glucose unit forming a radical, which in turn reacts with the ferric ion, and finally with hydrogen peroxide [24, 21]:



If the reaction is carried out to completion, then ultimately the organic molecules break down into CO₂ and water. If the pH is too high the iron can be precipitated as Fe(OH)₃ and at high pH H₂O₂ can decompose to oxygen and water. However, the homogeneous, water soluble FePcS catalyst does not precipitate at high pH and can thus be used in basic environment.

3.2 Results obtained from H₂O₂ decomposition

The decomposition of H₂O₂ was investigated under the following conditions: self-decomposition, decomposition in the presence of starch, decomposition in the presence of the catalyst and finally, in the presence of both starch and the catalyst. The decomposition of hydrogen peroxide was found out to be highly dependent on the pH (see Table 3.1). Hydrogen peroxide alone showed very slow decomposition at 55 °C and pH 5. When adding NaOH the decomposition increased; at pH 8.6 the yield (recovered solid starch) was 58 % after 24 h, and at pH 10 the yield was only 36 % after 8 h and 0% after 24 h, respectively (Table 3.1, entries 1-3b) . Without a catalyst, there is no or hardly any carboxyl groups formed, see entries 4-6. In the presence of

FePcS catalyst, H_2O_2 decomposes more rapidly, and the rate is increasing with increasing pH, see entries 7-10. Thus, if the solution is highly alkaline (pH=10), with the catalyst present all the H_2O_2 is decomposed in less than one hour, or without the catalyst 73% of the H_2O_2 has decomposed after 8 h, while hardly any starch oxidation have occurred. However, 33 % of the starch has decomposed at pH 10, see entry 6. Additionally, if having both the catalyst and starch at an initial pH level of 10 (see entry 13), all H_2O_2 is consumed while the carboxyl content is relatively low. DS was only 0.48 per 100 AGU units, while the solid starch yield had decreased to 87 %.

This can be explained by the fact that the H_2O_2 is decomposed too fast, partly degrading the starch. The most interesting observation was that when starting with an initial pH of 8.6 in the presence of both starch and the catalyst (see entry 12), all the starch (97 %) had become water soluble after 24 h. At the same time the pH had surprisingly dropped to 2.25 from the initial 8.6, indicating extensive carboxylic acid formation. There was 43 % H_2O_2 left after the reaction and the carboxyl content was 3.90 per 100 AGU.

3.3 Kinetic results of semibatch experiments

Based on results obtained in the preliminary experiments, the most feasible reaction conditions for starch oxidation were chosen for kinetic experiments. The catalyst was shown to be active under alkaline reaction conditions. Too strong H_2O_2 concentrations caused starch depolymerization, in addition since the H_2O_2 reactions (decomposition and starch oxidation) are exothermic it is safer to add small amounts of H_2O_2 continuously than the whole amount at once.

The kinetic experiments were performed under alkaline pH regime. The selected three pH levels were 7, 8.4 and 10. The carboxyl and carbonyl contents, as well as H₂O₂ and the gas evolution were determined. Carboxyl groups were formed at the highest rate at the highest pH 10 (Figure 3.1), but at the same time starch decomposed to low molecular weight products. After 7 h, the carboxyl DS was 1.7 per 100 AGU units, but 33 % of the starch was lost. When decreasing the pH, less COOH groups were formed compared to the experiment performed at pH 10, and the starch recovery was at a reasonable level (only 10 % solid starch lost at pH 8.6 and 5 % at pH 7, respectively).

Table 3.1. Preliminary experiments, reaction temperature 55 °C.

Entry	pH	t (h)	starch	catalyst	H ₂ O ₂ yield %	DS _{COOH} / 100 AGU	Solid starch yield %
1	5	24			98		
2	8.6	24			58		
3	10	8			34		
3b	10	24			0		
4	5	8	x		98	0	88
5	8.6	8	x		50	n.d.	n.d.
6	10	8	x		27	0.03	67
7 ^a	5	24		x	99		
8	5	8		x	97		
9	8.6	8		x	50		
10	10	1		x	0		
11	5	8	x	x	88	0	75
12	8.6	8	x	x	43	3.90	3 ^b
13	10	8	x	x	0	0.48	87
14	2	8	x	x ^c	51	n.d.	0

^a experiment at 20 °C

^b Solid insoluble starch was 3 % left, 77 % of water soluble starch recovered with acetone precipitation. Final pH 2.25.

^c FeSO₄ used as catalyst with AGU : cat molar ratio 10000:1; starch decomposed

The formation of carbonyl product showed a different behavior compared to the carboxyl formation at different pH levels (Figure 3.2). The highest formation of C=O groups was not found at the highest pH (10), but at pH 8.4. The formation of H₂O₂ hydroxyl radicals is probably higher at this pH level, while the decomposing reaction to water and oxygen is more prominent at pH 10 than at lower pH levels (compare Table 3.1, entry 10, 12), which could explain this phenomenon.

In both the carboxyl and carbonyl formation, there are clearly two separate phenomena. At the beginning (0-240 minutes), the products are mainly formed on the surface of the starch granules, while later (240-420 minutes) partial degradation allows reaction inside the granule and the reaction rate increases again.

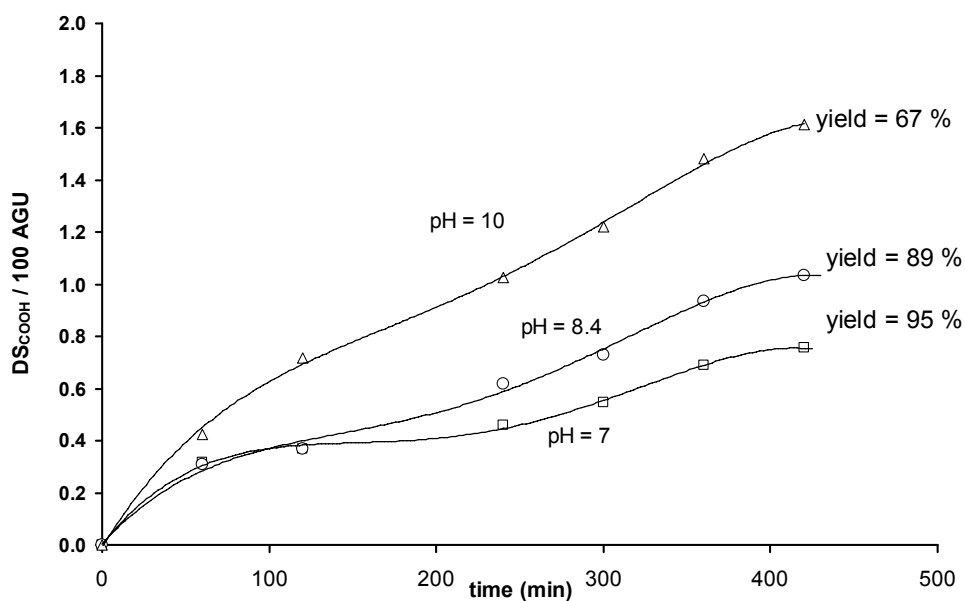


Figure 3.1. The kinetics of the carboxyl formation at different pH levels (7-10) when using AGU/cat ratio of 12000:1 and H₂O₂ flow of 22 ml/min at temperature of 55 °C. Yield corresponds to the amount of recovered solid starch at the end of the experiment.

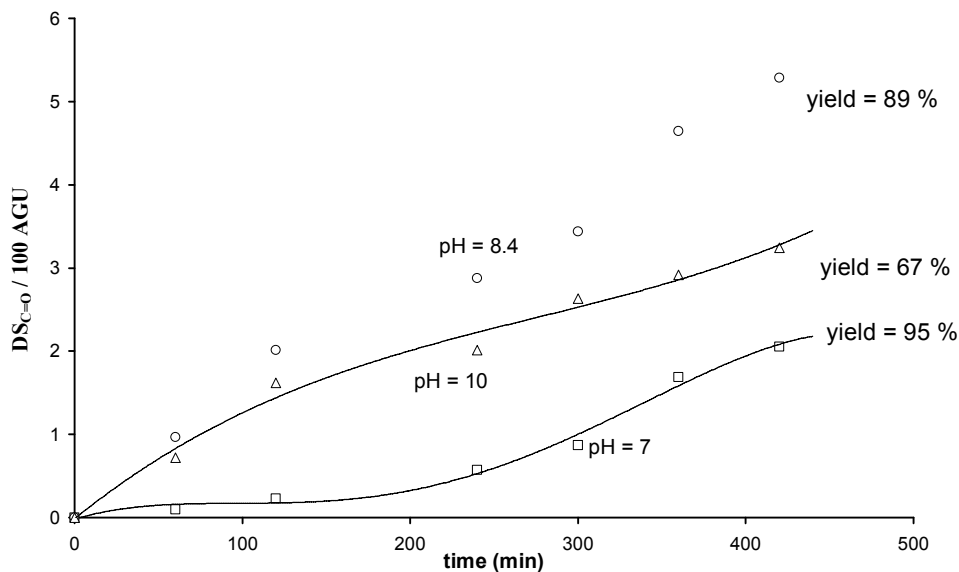


Figure 3.2. The kinetics of the carbonyl formation at different pH levels (7-10) when using AGU/cat ratio of 12000:1 and H₂O₂ flow of 22 ml/min at temperature of 55 °C. Yield corresponds to the amount of recovered solid starch at the end of the experiment.

The DS values achieved corresponds well to the DS values obtained in the previous studies at similar reaction conditions [18]. In Table 2 the performed kinetic experiments are compared with some results from the literature, which also employed hydrogen peroxide as an oxidant. At pH 7, DS_{COOH} = 1.85 and DS_{CO} = 5.46 were reported whereas in our study DS_{COOH} = 0.75 and DS_{CO} = 2.05 (Table 2, entry 3 and 5) are recorded. The slightly lower values in our study can be explained by the fact that in the work of Sorokin et al. [18], the temperature was 58 °C compared to 55 °C in this study. A few degrees may in fact have a considerable influence meaning that the reaction temperature can be in the gelatinization zone or slightly below it. Moreover, in the current investigation samples were taken during the course of the reaction, influencing the solid to liquid ratio. When comparing the effect of the H₂O₂ flow rate, it can be noticed that when reducing the flow by half,

also the DS_{COOH} is reduced by the same amount while DS_{CO} is reduced by 2/3 (Table 3.2, entries 2 and 4).

Table 3.2. Comparison of performed kinetic experiments and DS values from the literature.

Entry #	Reaction conditions				DS_{COOH}	DS_{CO}	Yield ^a	Ref.
	T (°C)	pH	H ₂ O ₂ flow	catalyst	/100AGU	/100 AGU	%	#
1	55	10	22	FePcS	1.61	3.24	67	[8]
2	55	8.4	22	''	1.03	5.28	89	[8]
3	55	7.0	22	''	0.75	2.05	95	[8]
4	55	8.4	11	''	0.46	1.87	96	[8]
5 ^b	58	7		''	1.85	5.46		[18]
6 ^c	58	3		FeSO ₄	0.00	0.00		[18]
7 ^d	40	10		''	0.90	6.40	91	[24]
8 ^e	40	acidic		''	0.59	0.87		[33]
9 ^f	90	2.0		WO ₄ ²⁻	24.4	-		[19]

^a Yield = total amount of recovered solid starch

^b Reaction temperature 58 °C, FePcS as catalyst AGU / catalyst ratio = 12900 : 1, reaction time 7 h, hydr. per. flow equivalent to entry 4.

^c Reaction temperature 58 °C, FeSO₄ as catalyst, AGU / catalyst ratio = 644 : 1, reaction time 7 h, hydr. per. flow equivalent to entry 4.

^d Reaction temperature 40 °C, FeSO₄ amount 0.1 w-% based on dry starch, reaction time 4 h, hydr. per. added in beginning of experiment.

^f starch gelatinized and reaction performed at 90°C.

As can be seen (Table 3.2, entry 6), if using FeSO₄ with the same AGU / catalyst ratio as FePcS, no starch oxidation occurs [18]. If the reaction temperature is high and gelatinization is allowed, then it is possible to achieve much higher substitution degrees (entry 9), since the reaction solution have higher surface contact with the starch. In contrast to the result obtained in the H₂O₂ decomposition experiments (Table 3.1), maintaining the pH at 8.4 with pH stat does convert the starch into soluble starch as it was in the case of only adjusting *initial* reaction media to pH 8.6 (Table 3.1, entry 12). The pH dropped to a final 2.25 due to formation of low molecular carboxylic acids. The solid starch was heavily depolymerized (as can be

seen in SEM analysis, Figure 3.6), thus increasing the surface area, which could explain the high DS_{COOH} in this experiment.

The oxygen evolution could be determined by observing the H_2O_2 added to the reactor, and H_2O_2 concentration in the reactor at specific reaction time (by titration of samples), by monitoring the gas flow out of the reactor and analyzing it by MS. The results of the oxygen evolution can be seen in Figures 3.3 and 3.4 at two different pH values, 8.4 and 10, respectively. At pH 7, the gas formed was too small to be detectable. At pH 8.4 the oxygen mass balance is substantially different compared to pH 10. The H_2O_2 is accumulated in the reactor to a final level of 0.8 mol/L and then maintained at that level, while the gas evolution starts to increase in the final phase of the experiments. At the pH level of 10, the H_2O_2 is not accumulated at all but remains at very low level during the experiment (see Figure 3.4).

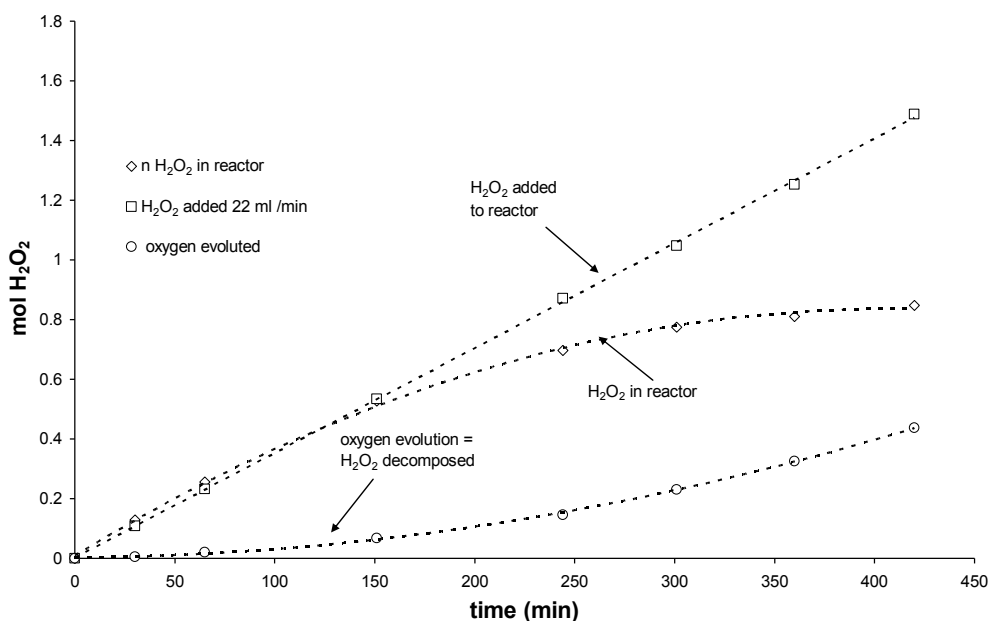


Figure 3.3. Hydrogen peroxide evolution at pH 8.4 when using AGU/cat ratio of 12000:1 and H_2O_2 flow of 22 ml/min at temperature of 55 °C.

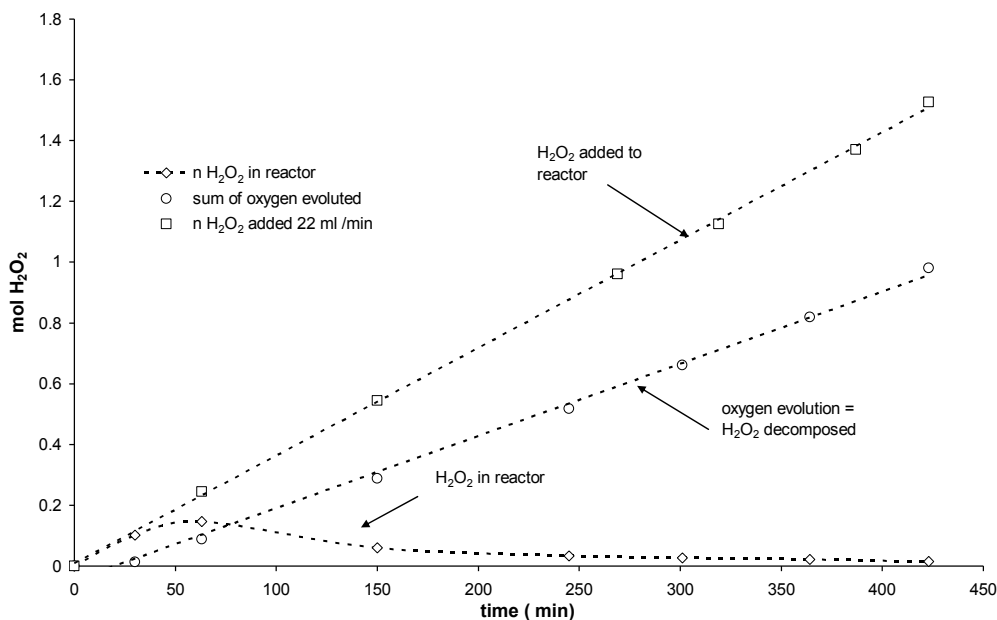


Figure 3.4. Hydrogen peroxide evolution at pH 10 when using AGU/cat ratio of 12000:1 and H₂O₂ flow of 22 ml/min at temperature of 55 °C.

The part of the starch that was decomposing and reacting further to low molecular compounds was found to be of a significant level when the pH was 10 (33 % of the solid starch was lost). The loss of the solid material can be seen during the experiment at pH 10 (Figure 3.5). Both the theoretical and the observed ratios were decreased due to the fact that solid starch was withdrawn and liquids were fed in, however, there was a clear difference between experimental and theoretical values. The experimental ratio was 29 % lower than the theoretical ratio at the final sample, which was in a good agreement with the total solid starch loss of 33 wt-% (= 67 % solid starch yield).

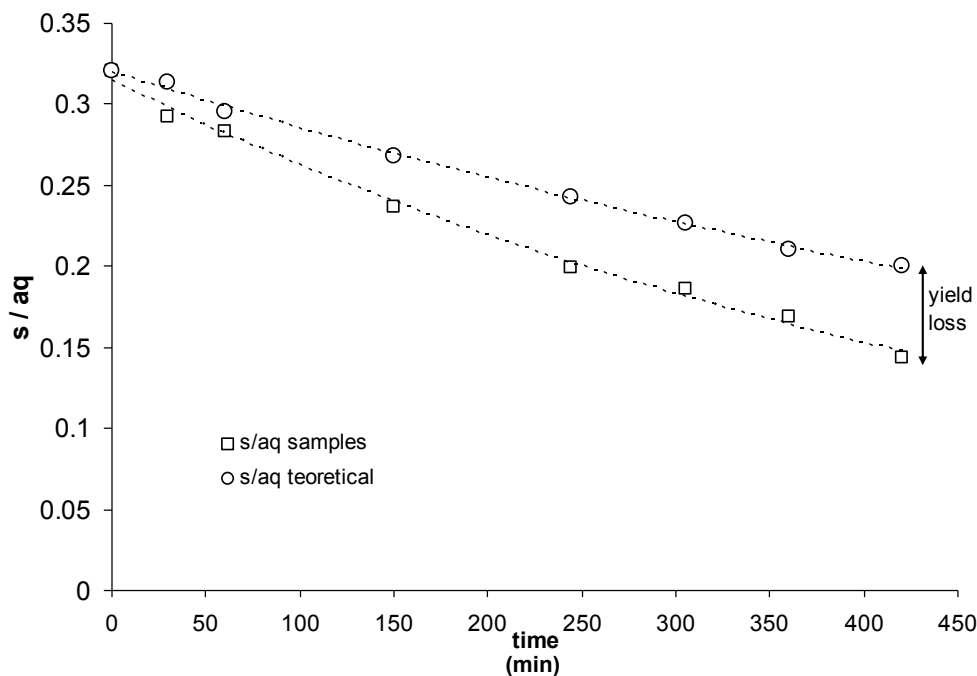


Figure 3.5. Theoretical and experimental values of solid to liquid ratios as a function of time. Reaction conditions: pH = 10, T = 55 °C.

Carbon dioxide (CO₂) can be formed by a terminal glucose oxidation route via decarboxylation, producing CO₂ [19]. The outlet gas composition was analyzed in this work online with MS. The only gas at pH 8-10 was oxygen, while no CO₂ was detected. In a comparable experiment with FeSO₄ as a catalyst using pH 2.8-3.0, only CO₂ was observed and no O₂. Clearly there was no terminal glucose oxidation occurring at the experiments performed in the alkaline solution with FePcS as the catalyst, but only internal glucose oxidation, which in turn formed low molecular compounds (such as erythronic, glyoxylic and formic acids).

3.4. Granular structures and residual iron content by SEM-EDXA – semibatch experiments

The structure of the oxidized starch granules is important. Although some applications allow the starch granules to be destroyed or gelatinized during oxidation, usually this is not the case. Thus the solid starch product was analyzed with scanning electron microscopy (Figure 3.6).

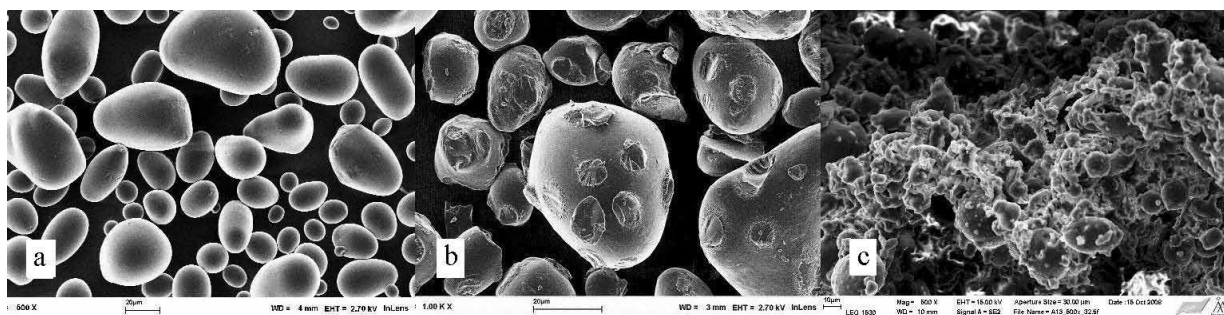


Figure 3.6. SEM pictures of **a)** native potato starch, **b)** oxidized starch at pH 10, **c)** and water soluble starch (see Table 3.1, entry 12).

The microphotographs made with SEM show a loss of smoothness on the surface of the starch granules (Figure 9.b). When the starch is allowed to react further to water soluble starch (Table 3.1, entry 12), the major part of the granules is still intact, but clustered together (Figure 3.6c). When analyzed with SEM-EDXA, the residual iron content of the FePcS oxidized starch was too low to be detected, whereas oxidized starch obtained with FeSO₄ was measured to have up to 0.20±0.05 wt-% iron content.

When analyzed with ICP-MS, the iron content was measured to 2.1 mg/kg for native starch, 9.5-15.4 mg/kg (pH=8.4 and pH=10) for FePcS oxidized starch, and 292 mg/kg for FeSO₄ oxidized starch, respectively. Moreover, the color of the FePcS oxidized starch was white, whereas the FeSO₄ showed a light brown discoloration (see photos of the starch samples at section 3.15).

3.5 Kinetic results and discussion of batch mode experiments

The H₂O₂ decomposition and the degree of substitution (DS_{COOH}, calculated on 100 AGU) results as well as the solid starch yields and initial reaction rates are collected in Table 3.3. Entries 1-3 are batch mode experiments at three different pH values, entry 4 is an experiment with a catalyst solution feed, entry 5 is an experiment with ultrasonically treated starch (section 2.4), and entries 6-8 are experiments performed at three different pH values in the semi-batch mode, i.e. H₂O₂ added continuously to the reaction mixture [8].

Table 3.3. Final degree of substitution (COOH, expressed by 100 AGU), the solid starch yield and the initial decomposition rate (r) of H₂O₂ for each experiment. Entries 6-8 are semi-batch experiments [8].

Entry #	Description	pH	Reaction time (min)	DS COOH / 100 AGU	$-r_{\text{H}_2\text{O}_2,0}$ mol/L*h	$r_{\text{COOH},0}$ COOH/100 AGU*h	Yield %	Ref.
1	batch	7.5	2640	0.45	0.006	0.08	87	[9]
2	batch	8.4	1560	0.35	0.045	0.14	82	[9]
3	batch	10	246	0.73	0.140	0.39	79	[9]
4	catalyst feed	8.4	1320	0.79	0.165	0.04		[9]
5	US - starch	8.4	1440	0.47	0.01	0.47	90	[9]
6	semi-batch	7	420	0.75	n.d.	0.30	95	[8]
7	semi-batch	8.4	420	1.03	n.d.	0.31	89	[8]
8	semi-batch	10	420	1.61	n.d.	0.40	67	[8]

^a The initial rate was calculated by the difference of initial concentration and first sample concentration divided by the time between the samples.

The batch mode experiments were performed at different pH (7.5, 8.4 and 10) by adding the catalyst and H_2O_2 in the beginning of the experiment.

3.5.1 Kinetic results

When adding the catalyst to the reaction mixture with a high concentration of H_2O_2 , a rapid decomposition of H_2O_2 was noticed. The decomposition stabilized in less than a minute. Therefore, the amount of decomposed H_2O_2 in the beginning can be considered negligible. These experiments were performed until there was no H_2O_2 left in the reactor. It is well known from the literature, that higher pH favours faster decomposition mainly via a dissociation step which generates a strong nucleophile – OOH peroxide anions, being able to further react with hydrogen peroxide resulting in decomposition products. As illustrated in Figures 3.7a and 3.7b, H_2O_2 was rapidly decomposed at high pH (10), and thus the experiment lasted only for four hours, whereas at a neutral pH (7.5), the experiment was continued for 42 hours (2500 min).

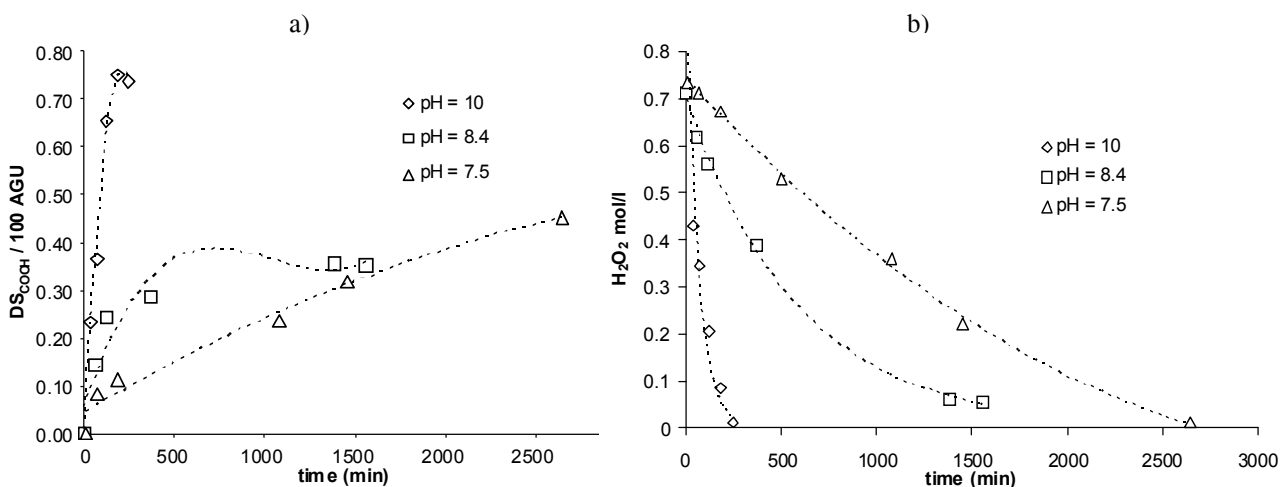


Figure 3.7. a) The effect of pH on the formation of carboxyl groups. 1b) the effect on pH on the decomposition of H_2O_2 .

The initial concentration of H_2O_2 was $0.70 (\pm 0.02)$ mol/l (=2.43 wt-%). The initial rate of the H_2O_2 decomposition was only 0.02 mol H_2O_2 /h at pH 7, compared to 0.09 mol H_2O_2 /h at pH 8.4 and 0.47 mol H_2O_2 /h at pH 10, respectively. The final degree of substitution was the highest at the highest pH. As can be seen from Figure 3.7a, the final degree of substitution of carboxyl groups ($t_r= 240$ min) was $\text{DS}_{\text{COOH}}= 0.73$ at pH 10, whereas it was 40 % lower ($\text{DS}_{\text{COOH}}= 0.45$, $t_r= 2640$ min) at pH 7.5. At pH 8.4, the lowest DS was found ($\text{DS}_{\text{COOH}}= 0.35$, $t_r= 1560$ min).

Even though a higher degree of substitution could be achieved in a shorter time at a high pH, the drawback of a high pH is the impaired yield of the solid starch that is recovered. When measuring the total amount of starch left after each experiment, 21 wt-% starch was lost at pH 10, whereas it was 18 wt-% at pH 8.4 and only 13 wt-% at pH 7.5. When comparing the yields in the semi-batch (Table 3.3, entries 6-8) and batch experiments, it can be observed that less starch is depolymerized in the former one than in the latter case. This can be explained by the fact that the semi-batch experiments lasted longer at high pH (240 minutes compared to 420 minutes for pH 10), since in the batch experiments H_2O_2 decomposes much faster due to the higher initial concentration.

3.5.2 Low molecular weight compounds

The analysis showed that the low molecular compounds mainly consisted of less than 10 compounds; for instance, hydroxyacetic acid (glycolic acid), ethanedioic acid (oxalic acid) and 2,3-dihydroxypropanoic acid, which were formed mainly at high pH 10, and lactic acid which is mainly formed at lower pH. Moreover, it can be considered that a large part of the low molecular products consist of formic acid (the final decomposition product). This conclusion should be further confirmed by HPLC, since formic acid is too volatile for GC analysis (it evaporates during N₂-evaporation). Additionally, around 30 other products were found, but with too low concentrations to be reliably identified.

3.5.3 Catalyst solution feed (Table 3.3, entry 4).

Previous studies gave reasons to suspect that the catalytic activity decreased during the experiments, probably due to the progressive degradation of the catalyst. The observed gradual disappearance of the blue color of the catalyst during experiments, especially at pH 8.4, could have been due to a degradation of phthalocyanine cycle. The fragmentation of the phthalocyanine ring in the presence of peroxides has previously been reported to lead to the formation of sulfophthalimide and metal complexes containing the resulting tridentate ligand by Alessandro et al. [34].

By feeding the catalyst into the reactor during the experiment, the catalyst deactivation can be studied in more detail. In total, 140 mg of the catalyst dissolved in

120 ml of water was fed at the rate of 12 ml/h (=14 mg cat./h). After the feed was completed, the experiment was continued until almost all of the H_2O_2 had decomposed. As can be seen from Figure 3.8, the decomposition of H_2O_2 is similar to the one achieved in a batch mode, at pH 8.4, although the initial H_2O_2 decomposition rate was faster in the batch mode compared to the semi-batch one. A comparison of the curves in Figure 3.8b reveals that the catalyst catalyzes the decomposition of H_2O_2 : the initial rate of the H_2O_2 decomposition is higher, when the whole catalyst amount is added instantaneously in the beginning of the experiment. When comparing the DS_{COOH} , a clear difference is visible; at around 500 minutes of reaction, the reaction rate is the highest in the catalyst feed experiment, whereas for the batch mode experiment, the rate has already declined or even halted completely. The final degree of substitution DS_{COOH} in a continuous mode was 0.79, being twofold higher than the one achieved in standard the batch mode.

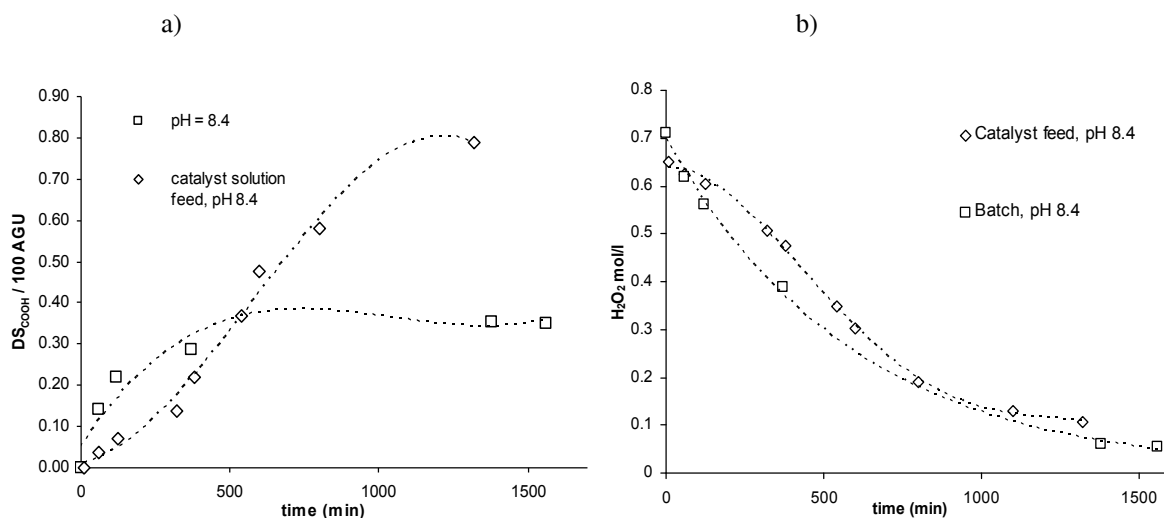


Figure 3.8. a) DS_{COOH} when feeding the catalyst solution continuously into the reactor (12 mg cat./h), b) the concentration of H_2O_2 . The results are compared with a standard batch experiment at pH 8.4.

3.5.4 Ultrasound-pretreated starch

Native potato starch was pretreated with ultrasound (see Section 2.4) in an aqueous solution to study whether the ultrasonic irradiation produces some pores or cavities in the starch granules and, therefore, leads to a higher degree of substitution (Figure 3.9). The starch (280 g) was dried after the ultrasonic treatment and 5 grams (1.7 wt-%) of the starch was found to be lost due to the ultrasound. In the starch oxidation, a 60 % higher DS was achieved starting from ultrasound treated than from non-treated starch (Figure 3.10). The native potato starch had a specific surface area $10 \text{ m}^2/\text{g}$ (Figure 3.9), while the ultrasound-treated starch had a specific area $18 \text{ m}^2/\text{g}$, indicating that ultrasound had by sonophysical effect created additional pores in the starch granules. There is also a possibility of a contribution of grounded starch particles. Therefore, particle-size analysis was performed for native potato starch and ultrasound-treated potato starch with a laser diffraction particle-size analyzer (device Malvern Instruments, model 2601Lc). The lens which was used limited the analysis to particles under $100 \text{ }\mu\text{m}$. It was found that the distribution of particles did not change substantially, but, in fact, the mean particle size even increased, see Figure 3.11 below. The reason for this could be that the ultrasound defragmented the surface of the granules, increasing the surface roughness, which might lead to agglomeration of particles. Another explanation for the particle-size distribution after the ultrasound treatment could be swelling.

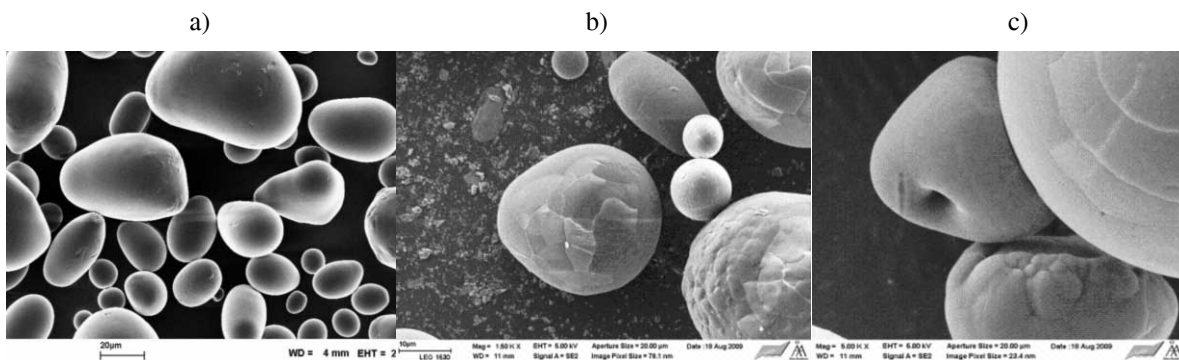


Figure 3.9. **a)** Native potato starch (BET: $10 \text{ m}^2/\text{g}$, zoom 500x), **b)** native potato starch treated with ultrasound 24 hours at $38 \text{ }^\circ\text{C}$, (BET: $18 \text{ m}^2/\text{g}$, zoom 1500x), **c)** ultrasound treated starch after reaction in $\text{pH} = 8.4$ (zoom 5000x).

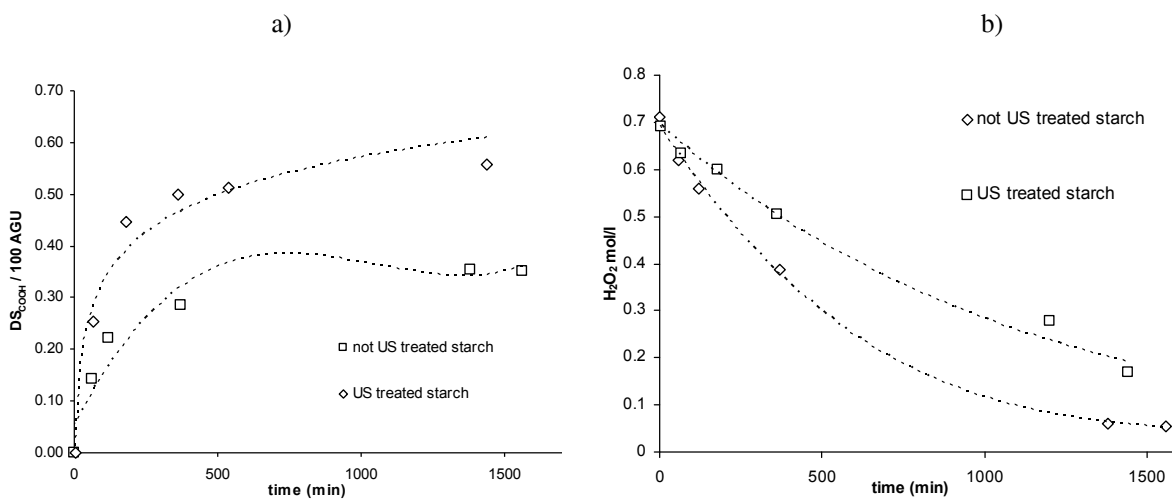


Figure 3.10. **a)** DS_{COOH} when pretreating the starch by ultrasound, **b)** the concentration of H_2O_2 . Results are compared with the standard normal batch experiment without starch pretreatment at $\text{pH} 8.4$.

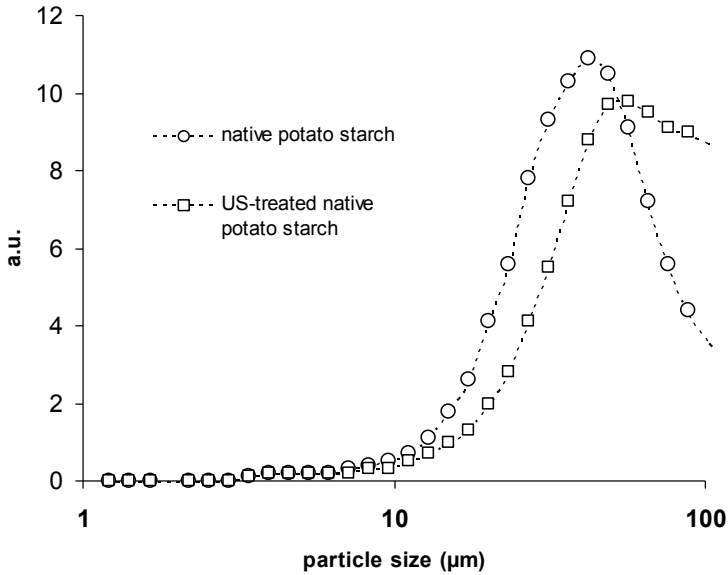


Figure 3.11. Particle size distribution analysis for native potato starch and ultrasound treated potato starch. $D[0,5]_{\text{native}} = 39 \mu\text{m}$; $D[0,5]_{\text{U.S. treated}} = 52 \mu\text{m}$.

The H_2O_2 decomposition was found to be slower with the ultrasound pre-treated starch than in the case of using native starch. The reason for this could be that the ultrasonic treatment partially dissolved the amorphous fractions of the starch granules, which in turn were washed away when filtering the pre-treated starch. This amorphous part may be the one that is more prone to be depolymerized to low molecular weight compounds (sugar acids) than the native starch. A large part of the H_2O_2 is then used for these “unnecessary” oxidation reactions. This can be more closely studied by changing the amylose-to-amylopectin ratio of the native starch and analyzing the ultrasonically treated starch by a photometric method [35].

3.5.5 Reaction mechanism

The plausible reaction mechanism for starch oxidation is described in Figures 3.12-3.13

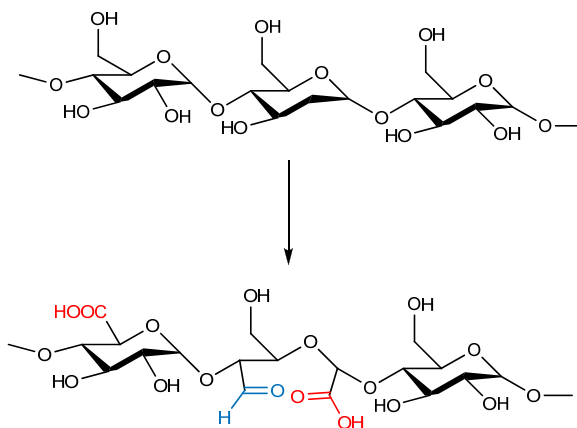


Figure 3.12. Overall reaction scheme for starch oxidation: carboxyl (red) and carbonyl (blue) groups are formed on different locations of the anhydroglucose unit; C2-C3 cleavage produces dialdehyde or aldehyde-carboxyl combination, whereas oxidation of the C6 produces a carboxyl group.

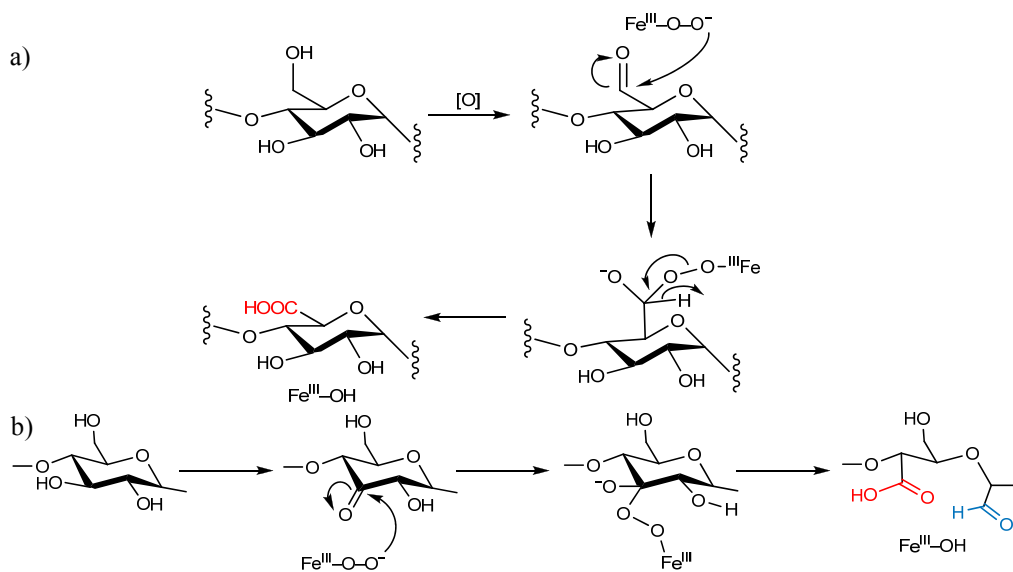


Figure 3.13. Detailed reaction mechanisms for **a)** carboxyl group formation at position C6, **b)** carbonyl and carboxyl group formation by C2-C3 bond cleavage.

3.5.6 H₂O₂ decomposition studies

The decomposition of H₂O₂ in the absence of starch was found out to be slightly slower than in the presence of starch, as can be seen from Figure 3.14a. The effect of the temperature on the decomposition of H₂O₂ was clear as revealed by Figure 3.14b. The activation energy was calculated to be around 117 kJ/mol.

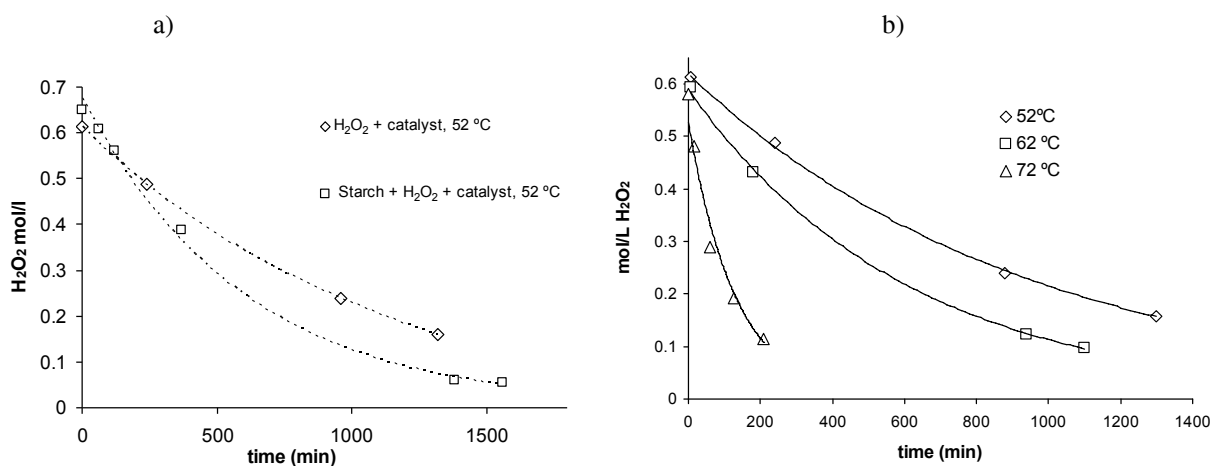


Figure 3.14. a) The decomposition of H₂O₂ with or without starch at pH 8.4, b) the effect of temperature on the catalytic decomposition of H₂O₂, at 52, 62 °C and 70 °C at pH 8.4.

It should be mentioned, that H₂O₂ can be classified as a weak acid, acting as a buffer. Therefore, the decomposition of H₂O₂ will inevitably increase the pH during the experiments: the final pH of the experiments was not 8.4 but closer to 9. This is, however, a small increase only. Kinetic modeling of the H₂O₂ decomposition was performed by using the data recorded at these three temperatures.

3.5.7 Modeling of H₂O₂ decomposition

Preliminary kinetic modeling was performed to reveal the catalytic decomposition rate, activation energy and reaction order in more detail. As mentioned in a previous study [8], thermal decomposition is also occurring. At lower temperatures and pH, it can though be neglected, but already at moderate pH 8.6 at 55 °C, 10-15 % of the H₂O₂ had decomposed after 24h. In the presence of the catalyst at pH 8.4 and 52 °C, 84 % of the H₂O₂ had decomposed after 22h.

The parameter estimation was carried out by a special software MODEST [36]. The objective function θ was minimized by using a combined simplex and Levenberg-Marquardt algorithm [36]. This objective function was defined as follows

$$\theta = \sum (y_i - \hat{y}_i)^2 \quad (3.1)$$

where y_i is the experimental value and \hat{y}_i is the estimated value (here: concentration).

The coefficient of determination R^2 of the kinetic models is defined as follows [36]

$$R^2 = 1 - \frac{\sum (y_i - \hat{y}_i)^2}{\sum (y_i - \bar{y}_i)^2} \quad (3.2)$$

where y_i is the experimental value (the concentration), \hat{y}_i is the estimated value, and \bar{y}_i is the mean value of the observations.

The rate constant was defined as

$$k = k_o * \exp\left(\frac{-E_a}{R} \left(\frac{1}{T} - \frac{1}{T_{ave}}\right)\right) \quad (3.3)$$

where T_{ave} is the average temperature of the experiments (see Notation). Three different models were tested, first order, second order and a power law model. The empirical kinetics can be represented in the following way:

$$r = \frac{d[\text{H}_2\text{O}_2]}{dt} = -k[\text{H}_2\text{O}_2]^\delta \quad (3.4)$$

where δ is 1, 2 or an adjustable parameter. The ODE (eq. 3.4) was solved numerically during parameter estimation. For first order kinetics ($\delta = 1$), the parameter estimation gave the value of degree of explanation 88.48 % and the values of parameters $k_0 = 0.0028 \text{ min}^{-1}$ and $E_a = 103 \text{ kJ/mol}$. The second order model ($\delta=2$) was able to explain the experimental data with a degree of explanation 91.13 % and the values of parameters became $k_0 = 0.0079 \text{ (L/mol) min}^{-1}$ and $E_a = 110 \text{ kJ/mol}$. For the power-law model kinetics, the degree of explanation was 92.15 % with the statistical data shown in Table 3.4. This model gave the most accurate description as illustrated in Figure 3.15. The difference between the second order and general power law fit was, however, minor.

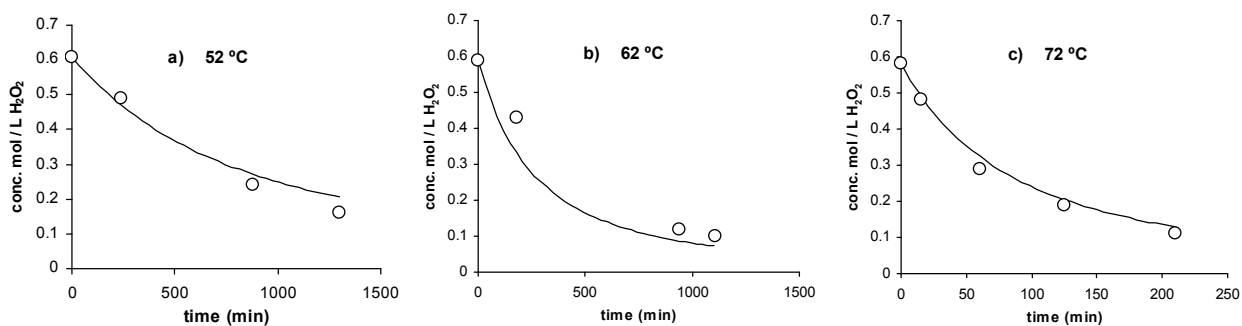


Figure 3.15. Modeling results of the catalytic decomposition of hydrogen peroxide at the temperatures **a)** 52 °C, **b)** 62 °C, and **c)** 72 °C.

Table 3.4. Estimated parameters with statistics; k_0 = rate constant at average temperature, E_a = activation energy, δ = reaction order.

Parameter	Value	std. error	relative std. error (%)	parameter/std. error
$k_0 / (\text{L/mol})^{\alpha-1} \text{min}^{-1}$	0.0053	0.0019	35.5	2.8
$E_a / (\text{kJ/mol})$	108	10.3	9.5	10.5
δ	1.6	0.328	20.5	4.9

To obtain a deeper insight in the decomposition process in the reaction environment, experiments were carried out under similar conditions, but in the absence and in the presence of the catalyst. The results are shown in Figure 3.16.

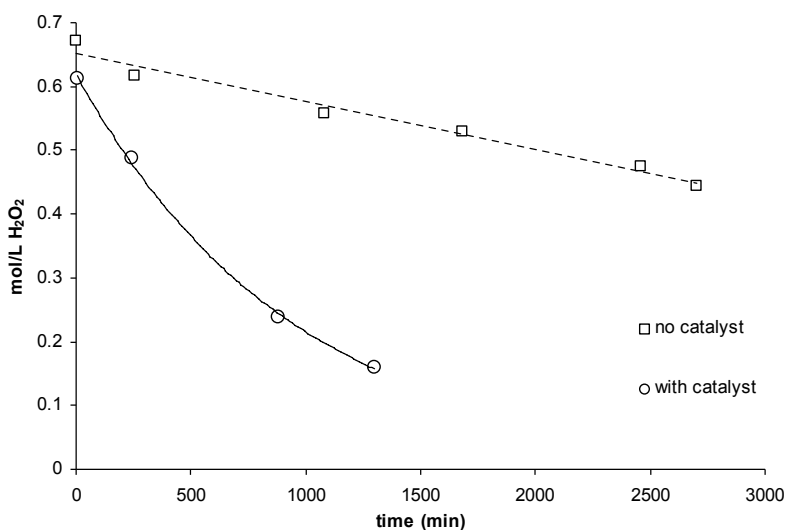
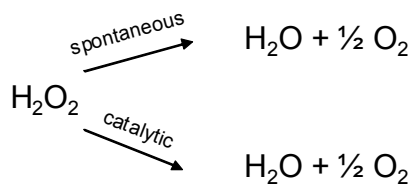


Figure 3.16. The decomposition of H_2O_2 with or without catalyst at $52\text{ }^\circ\text{C}$ and pH 8.4. According to Figure 3.16, the presence of the catalyst enhances the decomposition rate of H_2O_2 . Thus, a parallel decomposition pattern was assumed,



Based on this scheme, the following rate expression was used,

$$r = \frac{d[\text{H}_2\text{O}_2]}{dt} = -k_{\text{spo}}[\text{H}_2\text{O}_2]^2 - k_{\text{cat}}[\text{H}_2\text{O}_2]^2 \quad (3.5)$$

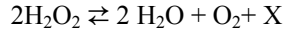
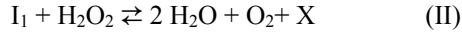
The reaction order was fixed to two because it gives better statistical response – the overall reaction order two gave a rather good fit in the preliminary modeling. The rate constant of the non-catalytic decomposition in the absence of the catalyst (k_{nonc}) was determined from the upper curve in Figure 3.16, after which the lower curve in Figure 3.16 was used to determine the influence of the catalyst on the decomposition rate. In the model, k_{cat} is, of course, dependent on the catalyst concentration, de facto $k_{\text{cat}} = k_{\text{cat},0} c_{\text{cat}}$. The estimated parameters for the non-catalytic decomposition are presented in Table 3.5. The degree of explanation was 94.49 %. At the second stage, in the presence of the catalyst, the values of k_{nonc} was kept fixed, to determine k_{cat} . The parameter values are given in Table 3.5. The degree of explanation was 90.05 %. According to reported literature, the value of k is equal to $9.255 \cdot 10^{-5} \text{ Lmol}^{-1}\text{s}^{-1}$ at $22.5 \text{ }^\circ\text{C}$ [37]. This value was obtained by using iron (II) as a catalyst. In our case by using eq (3), k_{cat} is equal to $9.92 \cdot 10^{-5} \text{ Lmol}^{-1}\text{s}^{-1}$ which is in the same range of magnitude as the reported one. Although iron (II) was used in both cases, the

complexity of our catalyst is much higher due to the presence of ligands, which can explain small difference in the rate constants.

Table 3.5. Estimated parameters and statistical data for the decomposition of H₂O₂ at 52 °C and pH 8.4.

Parameters	Estimated parameters	Estimated relative std. error (%)
$k_{0,\text{nonc}}$ (Lmol ⁻¹ ·min ⁻¹)	$0.40 \cdot 10^{-3}$	6.8
$k_{0,\text{cat}}$ (Lmol ⁻¹ ·min ⁻¹)	$6.0 \cdot 10^{-3}$	12.7

The H₂O₂ decomposition in the actual reaction environment is a complicated process. H₂O₂ decomposes to some degree spontaneously in the aqueous environment (Figure 3.16) at the pH-values and temperatures used in the experiments. In addition, the presence of solid starch might contribute to the decomposition (Figure 3.14). The main contribution to the decomposition originates, however, from the catalyst, as revealed by Figures 3.15 - 3.16. The fractional reaction order (Table 3.4) observed in the data fitting can be explained by the catalytic reaction mechanism as follows. Let us assume that hydrogen peroxide forms first a complex (I₁) with the catalyst (X), after which another hydrogen peroxide molecule reacts with the complex; water and oxygen are liberated and the catalyst is regenerated. In a simplified form, the process can be described as a two-step mechanism as follows:



The peroxy nature of complexes similar to I_1 , has been discussed [38].

Application of the quasi-steady state principle [39] to steps I and II and taking into account the total balance for the catalyst ($c_{0X}=c_X+c_{I1}$) allows us to derive the rate equation, which becomes

$$r = \frac{k_1 k_2 (c_{\text{H}_2\text{O}_2}^2 - c_{\text{H}_2\text{O}}^2 c_{\text{O}_2} / K) c_{0X}}{(k_1 + k_2) c_{\text{H}_2\text{O}_2} + k_{-1} + k_{-2} c_{\text{H}_2\text{O}}^2 c_{\text{O}_2}} \quad (3.6)$$

where K is the equilibrium constant of the overall reaction, $K=k_1 k_2 / (k_{-1} k_{-2})$. The overall reaction can be regarded as irreversible, which means that $K \rightarrow \infty$ and $k_{-2} \rightarrow 0$.

The rate equation simplifies to the form

$$r = \frac{k_1 k_2 c_{\text{H}_2\text{O}_2}^2 c_{0X}}{(k_1 + k_2) c_{\text{H}_2\text{O}_2} + k_{-1}} \quad (3.7)$$

For a constant catalyst concentration and temperature, the following merged parameters can be introduced: $k' = k_1 k_2 c_{OX} / k_{-1}$ and $\alpha = (k_1 + k_2) / k_{-1}$. The rate equation becomes

$$r = \frac{k' c_{H_2O_2}^2}{1 + \alpha c_{H_2O_2}} \quad (3.8)$$

As equation (3.8) shows, the apparent reaction order can vary between 1 and 2, depending on the value of the parameter α . Thus the empirical rate exponent between 1 and 2 obtained in the regression is logical (Table 3.4). By starting from slightly different hypothesis for the reaction mechanism, rate expressions are obtained, in which the water concentration appears in the denominator of the rate equation. The increase of the water concentration at the end of the experiments is approx. 1.2 wt.-% assuming that all hydrogen peroxide is decomposed. Thus the water concentration in the system can be assumed to be constant and the rate equation obtains a form which is similar to eq. (3.8). A more extensive kinetic study is necessary to reveal the details of the hydrogen peroxide decomposition mechanism in the current system.

3.6 Effect of the catalyst concentration and the solid-to-liquid ratio

The experiments are summarized in table 3.6. The catalyst concentration was found to have a large impact on the H_2O_2 decomposition rate (Figure 3.17a). In the absence of the catalyst, the decomposition curve was linear, indicating zero order kinetics. The presence of starch itself affected the decomposition rate, as can be seen when from the experiment carried out with starch but without a catalyst – the decomposition was also merely linear, but H_2O_2 decomposed twice as fast as the H_2O_2 alone does, when being influenced by only the alkaline reaction media (pH 8.4) and elevated temperature (52°C). Already a small amount of catalyst (10 mg) enhanced the decomposition remarkably, and first order kinetics with respect to H_2O_2 was recognizable, however, even by adding four times more catalyst (40 mg), the decomposition rate did not increase much further, which indicates a low reaction order with respect to the catalyst.

The decomposition kinetics of H_2O_2 has a more straightforward behavior when only the catalyst is present, without starch. There is a huge difference between using 10 or 20 mg of catalyst, however, when doubling up further, the difference is less prominent, as revealed by the entries 12-16 in Table 3.6 for the respective initial decomposition rates. For the sake of comparison, an experiment with 12 g of corn starch (S/L ratio 1/3) was added to the graph to illustrate the inhibiting effect on the decomposition.

Table 3.6. Performed experiments and their initial decomposition rate calculated from the difference of the initial concentration and the concentration in the first sample, and the final degree of substitution of carboxyl groups, if it was successfully determined.

Entry #	Type of experiment	$-r_{\text{H}_2\text{O}_2}$ (mol / l*h)	NaOH (ml 1.0 M)
1	3/2 corn starch, 0 mg cat.	0.0215	1.622
2	3/2 corn starch, 10 mg cat.	0.0439	2.95 c
3	3/2 corn starch, 40 mg cat.	0.0970	1.554
4	1/1 corn starch, 40 mg cat.	0.0634	2,502
5	2/3 corn starch, 0 mg cat.	0.0100	0.900
6	2/3 corn starch, 10 mg cat.	0.0570	0.58 c
7	2/3 corn starch, 40 mg cat.	0.0920	0.928
8	1/3 corn starch, 40 mg cat.	0.0851	3,80
9	1/6 corn starch, 40 mg cat.	0.0760	1.67
10	1/12 corn starch, 40 mg cat.	0.0546	0.872
11	1/24 corn starch, 40 mg cat.	0.0802	0.546
12	no starch, 0 mg cat.	0.0185	0.118
13 ^a	no starch, 2 mg cat.	0.0195	0.112
14	no starch, 10 mg cat.	0.0822	0,198
15	no starch, 20 mg cat.	0.1006	0.360
16	no starch, 40 mg cat.	0.1347	0,360
17	3/2 pot. starch, 10 mg cat.	0.0387	3.00
18	3/2 pot. starch, 10 mg cat. pH 10	0.2102	3.2
19	3/2 pot. starch, 40 mg cat. pH 7.8	0.0516	3.43 b
20	3/2 pot. starch, 40 mg cat.	0.0640	1.95 c
21	2/3 pot. starch, 10 mg cat.	0.0497	2.438
22	2/3 pot. starch, 40 mg cat.	0.1097	0.936
23 ^b	2/3 pot. starch, 40 mg cat. US-treated	0.0498	1,620
24	1/3 pot. starch, 10 mg cat.	0.0380	1.942
25 ^c	1/3 pot. starch, 20 mg cat.	0.0434	1.786
26	1/3 pot. starch, 40 mg cat.	0.1081	4.570
27	1/6 pot. starch, 10 mg cat.	0.0348	0.726

^{a)} instead of 1.0 M, 0.2 M NaOH was used. The value was calculated to an equivalent amount.

^{b)} The potato starch was pretreated with ultrasound to create higher specific surface area [21].

^{c)} The carboxyl content was determined to 0.33 COOH/100AGU.

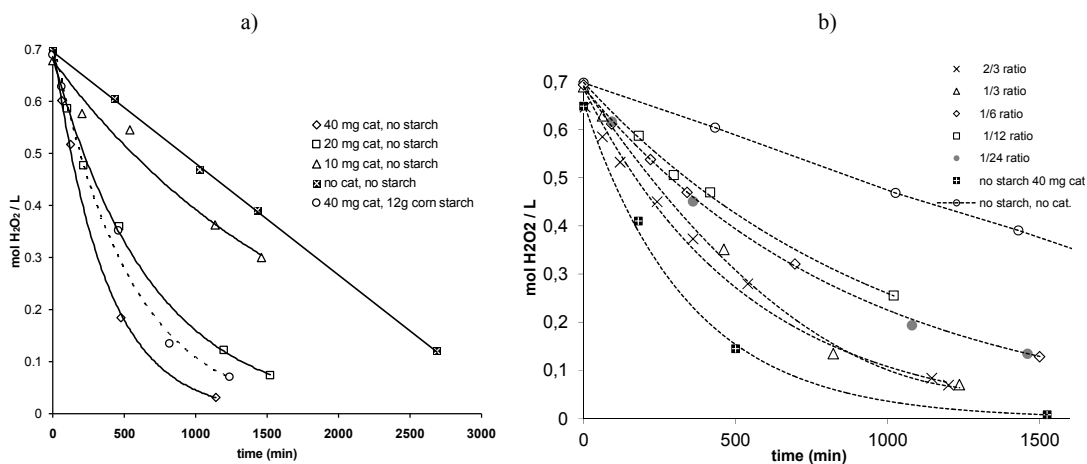


Figure 3.17. The decomposition of H_2O_2 **a)**, when without catalyst and starch, or with only 10, 20 or 40 mg of catalyst, compared with an experiment with 12 g of corn starch and 40 mg catalyst, and **b)** when alternating the corn starch solid-to-liquid ratio and 40 mg of catalyst. The pH = 8.4, T= 52 °C in all experiments.

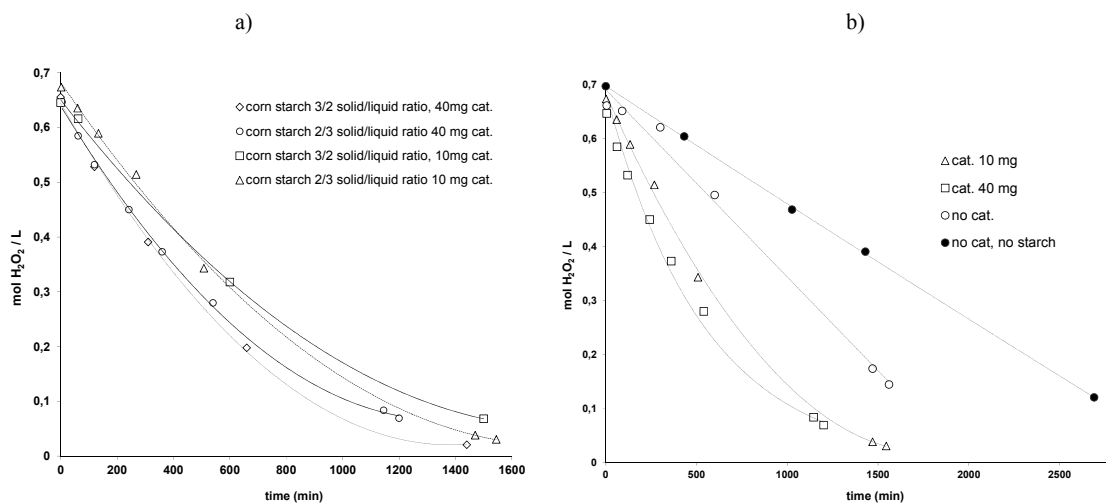


Figure 3.18. The decomposition of H_2O_2 when **a)** using corn starch with S/L ratio either 3/2 or 2/3 and the catalyst amount either 10 or 40 mg, and **b)** with fixed S/L ratio = 2/3 corn starch and using different concentrations of catalyst. The pH = 8.4, T= 52 °C in all experiments.

By altering the starch concentration (solid-to-liquid ratio, S/L) with a fixed amount of catalyst (40 mg), an interesting kinetic pattern was revealed. When a relatively large

amount of starch was used (S/L 3/2-2/3), the decomposition pattern seems to be a little more complex (Figure 3.17b), compared with the case with no starch but only catalyst. As illustrated, the experiment with the highest S/L ratio (2/3) falls into the middle of the curves, and the decomposition slows down when reducing the starch amount to 1/3, 1/6 and 1/12, but when decreasing the starch amount to 1/24, the decomposition rate increases again, and attains a maximum when no starch is present, but only the catalyst. In Figure 3.18a it can be seen that the effect of the catalyst amount is much more prominent than the effect of solid-to-liquid ratio. The catalytic decomposing effect of the starch itself, in turn, is revealed in Figure 3.18b, where no catalyst but only an amount of 2/3 corn starch is present – the decomposition is in fact more rapid than the case of 10 mg and no starch (Figure 3.17a). The initial decomposition rate as a function of the S/L ratio and with a fixed amount of the catalyst (40 mg) is illustrated in more detail in Figure 3.20b.

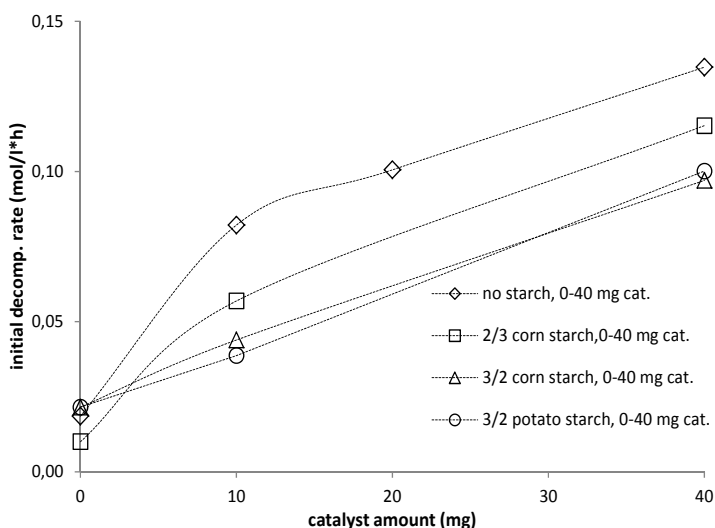


Figure 3.19. The initial decomposition rate of H_2O_2 at various S/L ratios (no starch, 2/3 and 3/2 ratios) as a function of the catalyst concentration. Temperature = 52 °C.

The influence of the catalyst amount (or in fact catalyst concentration since the same liquid amount was used in all experiments) on the initial decomposition rate is summarized in Figure 3.19 including four different S/L ratios. It is clear that the decomposition rate is increasing when decreasing the starch amount with all different catalyst amounts. Without the catalyst or using just a small amount of it, the decomposition rate seems to decrease with a non-linear pattern, whereas for the catalyst amounts 10-40 mg the rate seemed to increase rather linearly in all cases. There is no clear difference in the decomposition rates for potato starch compared to corn starch.

3.7 Effect of the starch origin

For potato starch instead of corn starch, slightly different decomposition trends were observed, when varying the catalyst concentration (Figure 3.20a) – compared to 10 mg of catalyst, 20 mg did not enhance the decomposition, whereas with 40 mg of catalyst, the decomposition rate was similar to that of corn starch with 40 mg catalyst (Figure 3.18a). In Figure 3.20b, the initial decomposition rates are displayed as a function of the S/L ratio for corn starch. On the secondary axis is shown, how the solid recovered starch yield changes as a function of the S/L ratio.

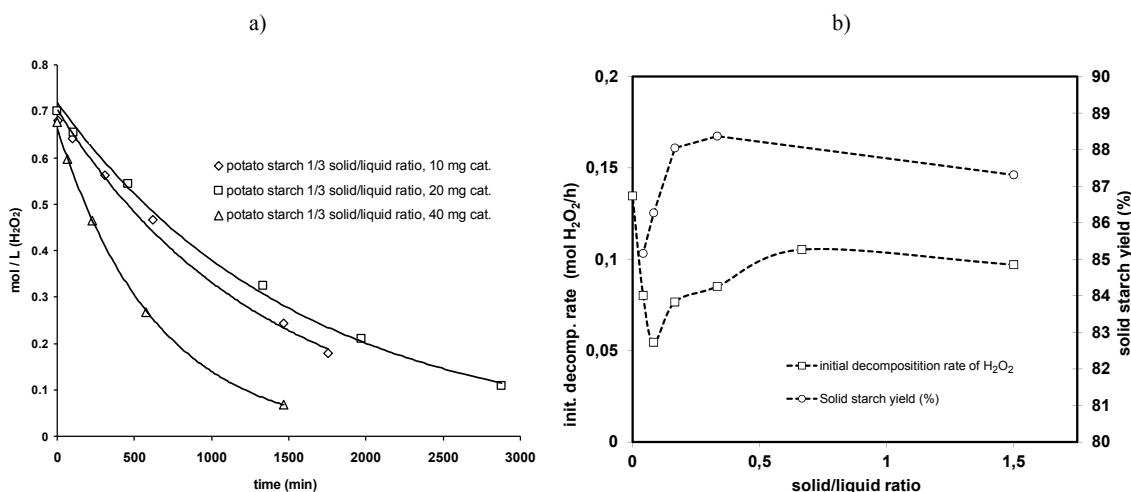


Figure 3.20. a) The decomposition of H_2O_2 when using potato starch and b) the effect of S/L ratio on initial decomposition rate and solid starch yield, when 40 mg catalyst is used, and $T = 52$ °C.

As can be seen, both the initial decomposition rate and the recovered starch yield remain moderately constant at higher S/L ratios (exceeding 1/3), but when approaching zero amount, differences become visible. The solid starch yield

drastically drops by almost 5 wt.-%, which can be explained by the large amount of H_2O_2 compared to starch which cause deterioration of the granules and a large amount is either dissolved or react to low molecular weight compounds. The initial decomposition rate again shows a minimum in the vicinity of the S/L ratio of 1/12, only being 0.05 mol/l*h, after which lowering the S/L ratio further gives an increase to 0.08 mol/l*h with the ratio 1/12, and eventually when decreasing the starch amount to zero, the decomposition rate exceeds 0.13.

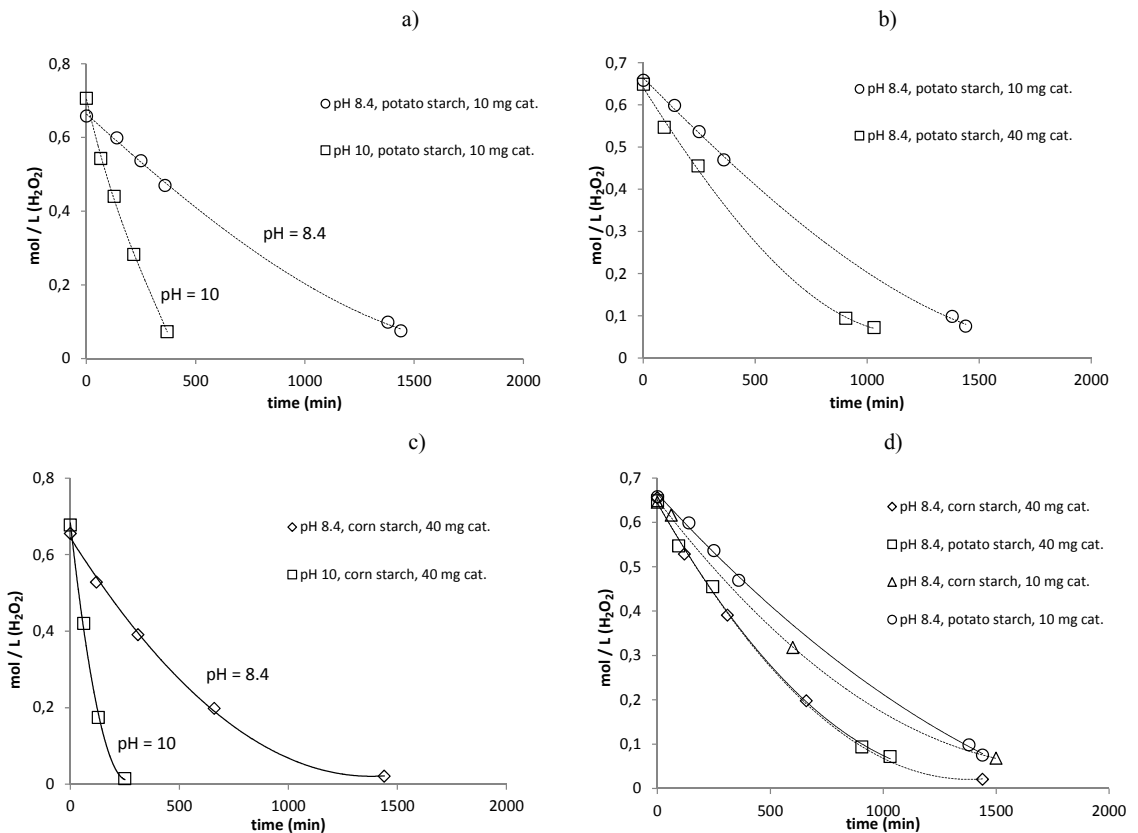


Figure 3.21. The decomposition rate of H_2O_2 when using the S/L ratio of 3/2 and **a)** potato starch, 10 mg of catalyst and pH 8.4 vs. 10, **b)** potato starch, pH 8.4 and catalyst amount 10 vs. 40 mg, **c)** corn starch, 40 mg catalyst and pH 8.4 vs. 10, and **d)** potato starch vs. corn starch, pH 8.4 and either 10 or 40 mg catalyst.

The influence of the pH (8.4 vs. 10) and the type of starch (potato vs. corn) are demonstrated by Figures 3.21a-d. It can be observed that the role of pH is more prominent than the catalyst concentration, in case of the decomposition of hydrogen peroxide. This is the case for both the corn and potato starch. In fact, the increase of the pH from 8.4 to 10 has a surprisingly large impact on the decomposition rate regardless of the catalyst amount– at pH 10 principally all H_2O_2 was decomposed after 400 minutes, whereas at pH 8.4 the time was 3-4 folds. Already a small increase of pH has a large impact on the decomposition as revealed by Figure 3.22.

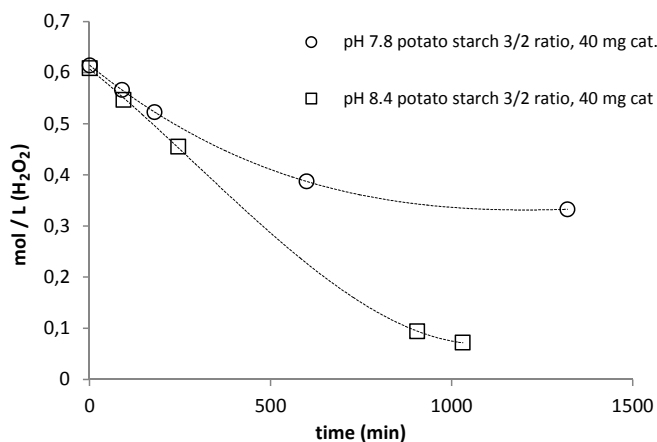


Figure 3.22. The decomposition of H_2O_2 when using potato starch with S/L ratio of 3/2, 40 mg catalyst at pH = 7.8 and pH = 8.4.

3.8 Effect of amylopectin and amylose contents

Corn starch with an essentially high amylopectin content may be the next big breakthrough in industry, since it has shown to have much better properties compared to normal potato or corn starch. Genetic modification of the potato has recently resulted in the development of a species containing only amylopectin (Amflora), and it soon becomes available for the industry. Since the Amflora is not yet available, unmodified waxy corn starch of high amylopectin content was used instead in an additional experiment.

The H_2O_2 decomposition in the presence of the high amylopectin starch is compared with high amylose starch in Figure 3.23. The pH=8.4, temperature of 52 °C and 40 mg of the catalyst (FePcS) were used in both experiments. The difference of the decomposition rates is evident; in the presence of amylose, H_2O_2 is decomposed much more rapidly, while in the case of amylopectin the decomposition rate was close to zero order and the initial decomposition rate was 3.5 times lower (0.155 vs. 0.042 mol/L*h).

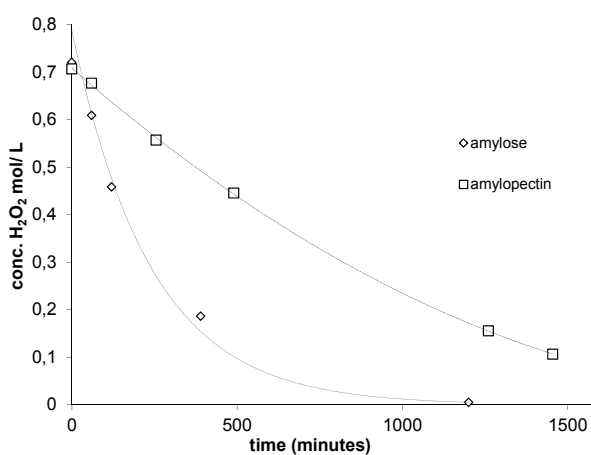


Figure 3.23. The H_2O_2 decomposition when oxidizing high amylose corn starch and high containing amylopectin corn starch at pH=8.4 and T = 52 °C.

3.9 Formation of carboxyl groups from S/L experiments

Since one of the goals of this study was to investigate how the available solid surface area of starch (and thus the S/L ratio) influences in the decomposition of H_2O_2 , only a minor effort was focused on the formation of the COOH groups during the oxidation process. It was found that there either a) was very little carboxyl groups formed in the case of corn starch, or b) the physical structure of corn starch prevents the reaction inside the granules, and therefore only very few carboxyl groups are formed, or c) there is some carboxyl group formation, but the standard analysis procedure by Smith's method was not able to detect the groups due to the high gelatination temperature of the starch which is needed for a successful titration.

Especially, in the case of high amylose corn starch, the gelatination prior COOH analysis was clearly not successful even though the starch solution was heated up to temperatures exceeding 90 °C. According to literature, this hypothesis is supported by the fact that to achieve full gelatination, over 110 °C is needed [40].

It was also noted that the acid washing which is needed prior to the gelatination for salt removal, did not influence the pH of the starch solution (pH was barely under 7, while for oxidized potato starch it is around 4). Therefore, it can be assumed that the physical structure of corn starch does not allow for carboxyl group formation, at least not inside of the granules.

3.10 Fragmentation of iron from the catalyst complex

It was observed that when using a very small amount (S/L ratio = 1/24), or no starch at all, brown solid residue was formed and attached to the reactor wall. The residue was most likely iron that had defragmented from the catalyst due to a too strong H_2O_2 concentration and lack of starch, a phenomenon that was observed already in a previous study where the decomposition of H_2O_2 under the influence of FePcS was studied [9]. A too strong H_2O_2 concentration in respect to the catalyst FePcS (over 10:1 molar ratio) has been reported to show a relatively fast and extensive demetalative fragmentation [34]. It is possible that the brown oxidized iron also appeared in experiments with starch present, however, in that case it formed complexes with the starch. Figure 3.24 shows the brown solid residue at the reactor wall from an experiment performed with no starch and 40 mg catalyst, at pH = 8.4 and T = 52 °C.



Figure 3.24. Brown solid residue can be observed on the reactor wall when using no starch.

3.11 Analysis of COOH and C=O concentrations of the solid starch by HPLC

The solid oxidized starch was hydrolyzed with perchloric acid and analyzed by HPLC. In Figure 3.25 it can be seen that carboxyl and carbonyl groups can be found by using this method. However, due to the low concentrations of the products it was more reliable to perform analysis by the titration methods. Dialdehyde starch was used for identification of the carbonyl peak.

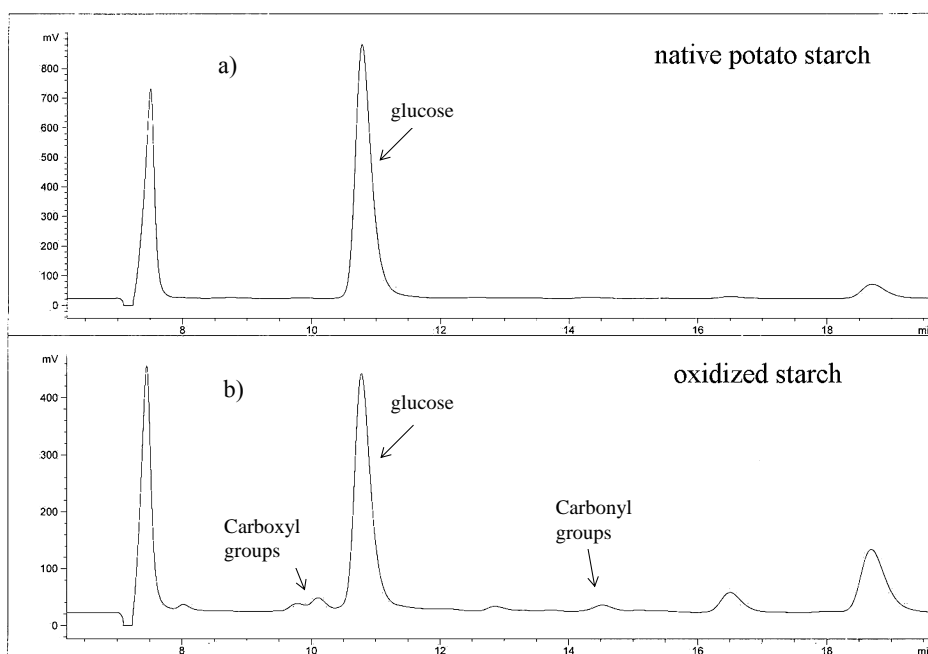


Figure 3.25. HPLC analysis of monomer units of **a)** hydrolysed native starch and **b)** oxidized starch.

3.12 Analysis of low molecular weight compounds by GC-MS

The aqueous phases of the oxidized starch samples were analyzed by GC-MS in order to identify qualitatively and if possibly, quantitatively, the low molecular weight products. As listed in Figure 3.27, products such as hydroxyacetic acid (glycolic acid), 2,3-dihydroxypropanoic acid (glyceric acid), ethanedioic acid (oxalic acid) were formed. The molecular structures of the most found compounds are illustrated in Figure 3.26 below.

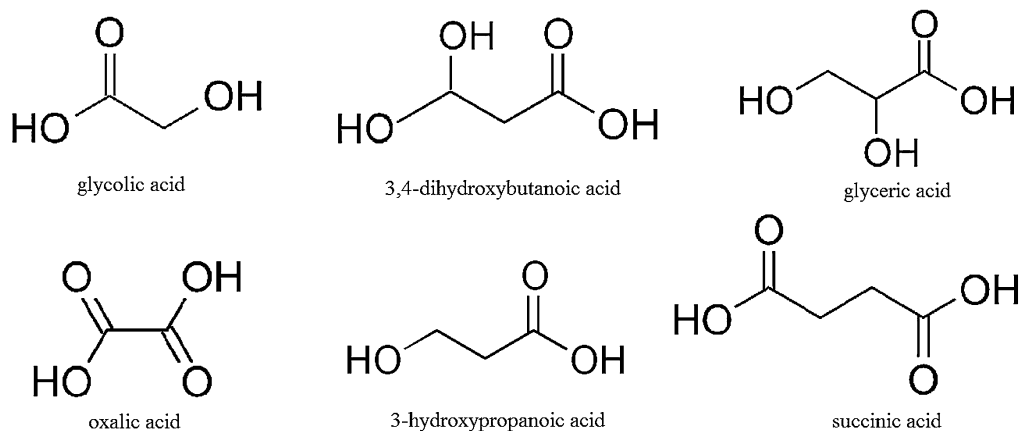


Figure 3.26. The molecular structures of the most abundant, identified, low molecular weight compounds found in the aqueous phase after starch oxidation when analyzed by GC-MS: Glycolic acid (50 wt.-%), 3-4-dihydroxybutanoic acid (9.6 wt.-%), glyceric acid (9.0 wt.-%), oxalic acid (2.3 wt.-%), 3-hydroxypropanoic acid (2.2 wt.-%), succinic acid (2.2 wt.-%).

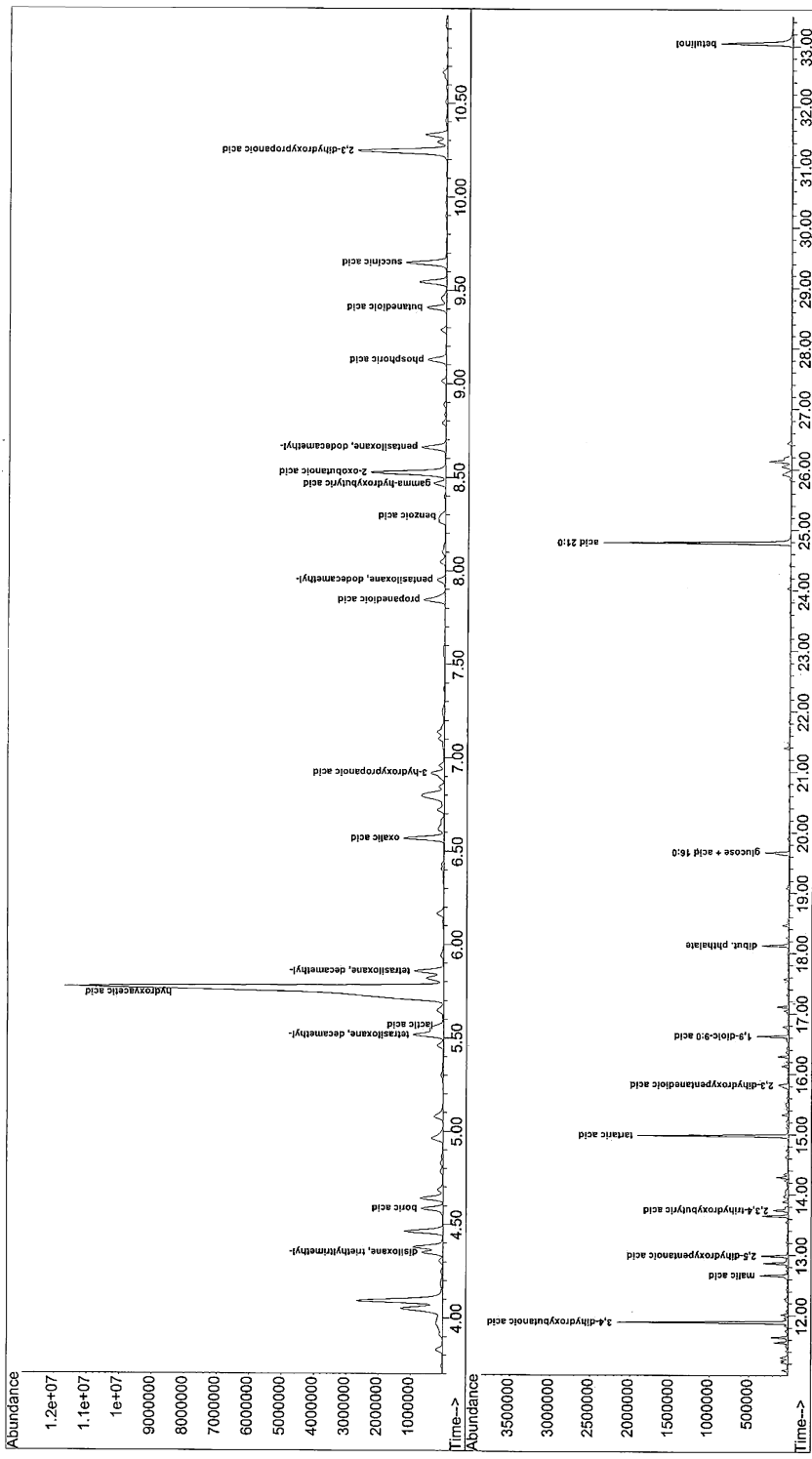


Figure 3.27. GC-MS analysis of low molecular weight products formed by starch oxidation.

3.13 Analysis performed with Q-TOF

The aqueous phase of some selected (experiment run at pH 7 and 10) end samples from the starch oxidation by FePcS catalyst and hydrogen peroxide were analyzed by Quadrupole time-of-flight mass spectrometer (Q-TOF-MS). Although the results were difficult to analyze due to a high amount of polymers (Figure 3.28), it was possible notice some trends. It was found out that hydroxyacetic acid (glycolic acid), ethanedioic acid (oxalic acid) and 2,3-dihydroxypropanoic acid were formed more at a high pH (10) than at a lower pH (7), while lactic acid was formed more at a lower pH. Moreover there were over 30 unidentified lower concentration compounds detected.

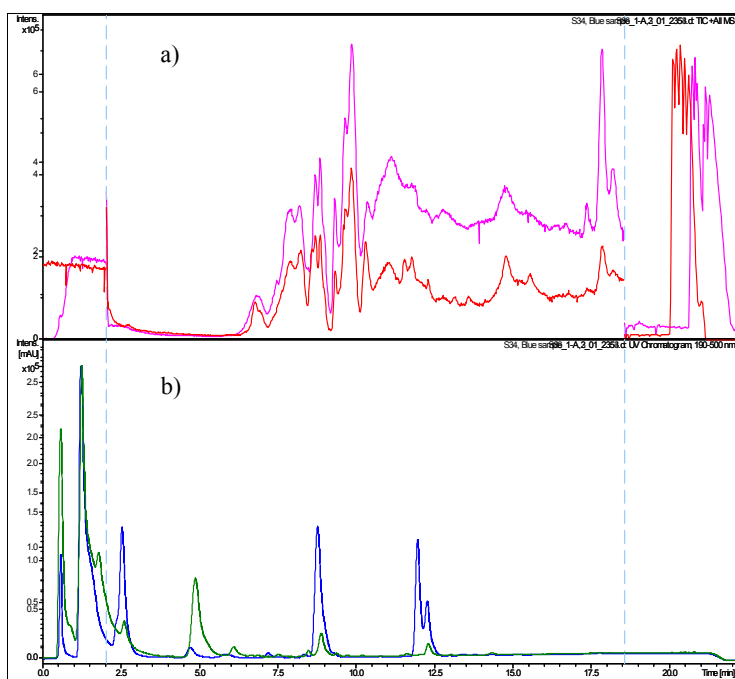


Figure 3.28. Q-TOF results. **a)** Total ion count (TIC), **b)** UV chromatogram. Red and green lines represent experiment with pH = 7, violet and blue with pH = 10.

3.14 Additional SEM analyses of solid starch samples

SEM images from selected native as well as oxidized or ultrasonically treated starch samples from different botanical origin are shown below in Figures 3.29-3.38. When comparing the native starch granules of potato starch with high amylose or high amylopectin corn starch, the difference in the granules average sizes as well as shapes are seen – potato starch granules are much larger and possess a spherical shape, whereas the corn starch granules are much smaller (note the different zoom) and more polygonal shaper, as already mentioned in Table 1.1.

The corn starches granules do not seem to be severely influenced by the oxidation in batch mode with hydrogen peroxide and FePcS, while in the case of potato starch, the granules seem to flocculate (bind to groups) and their surface is deteriorated (slightly at low pH, and much more at higher pH) and at both semibatch and batchmode . However, potato starch oxidized in batch mode did show slightly more deterioration and large holes were randomly observed on parts of the granules, probably due to the high initial concentration of H₂O₂.

Treatment with ultrasound created fracture-like surfaces on the potato starch granules. Further oxidation of the US-pretreated starch did not alter the granule surface significantly.

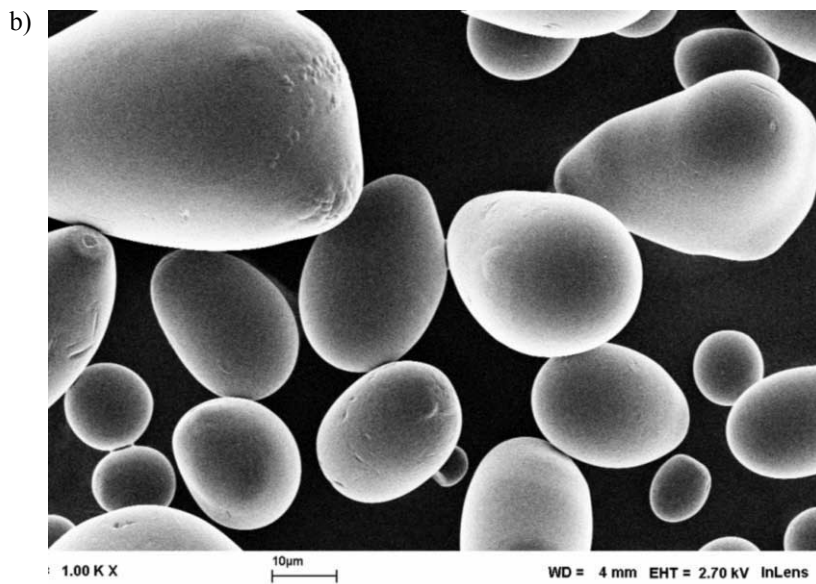
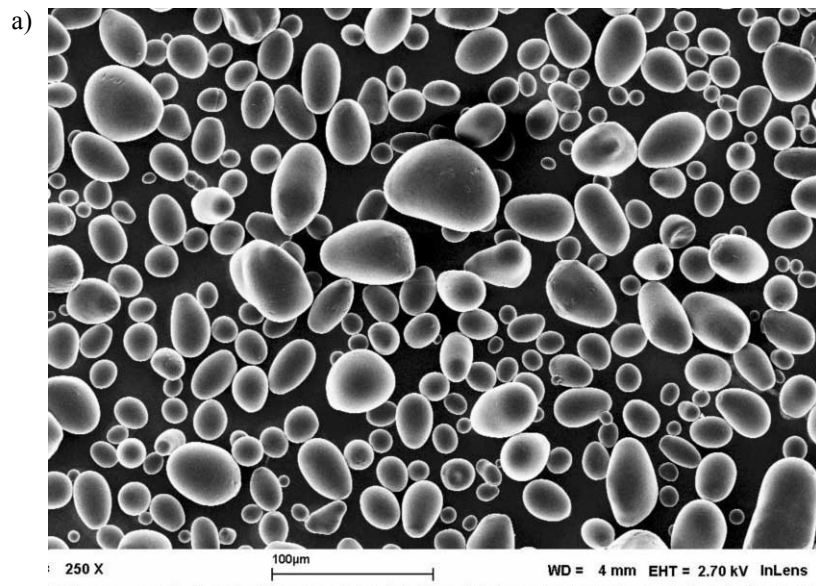


Figure 3.29. Native (unmodified) potato starch at **a)** 250x and **b)** 1000x zoom.

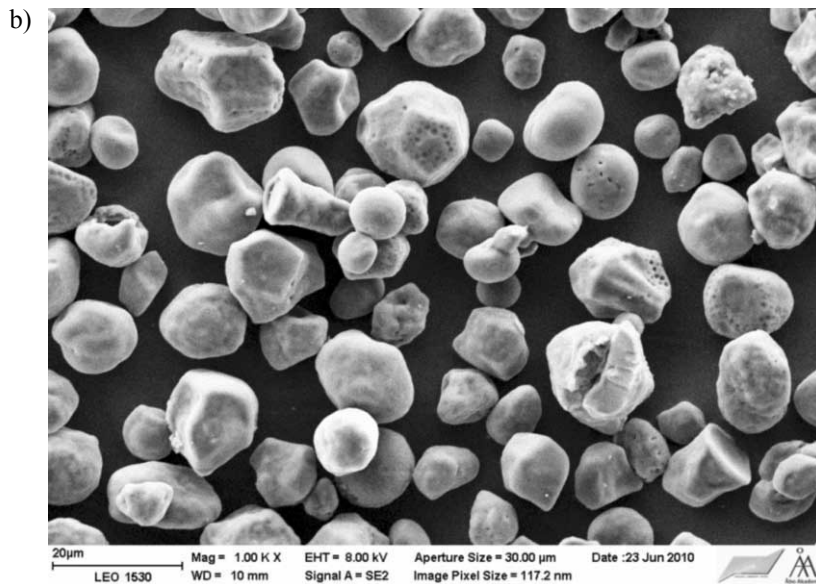
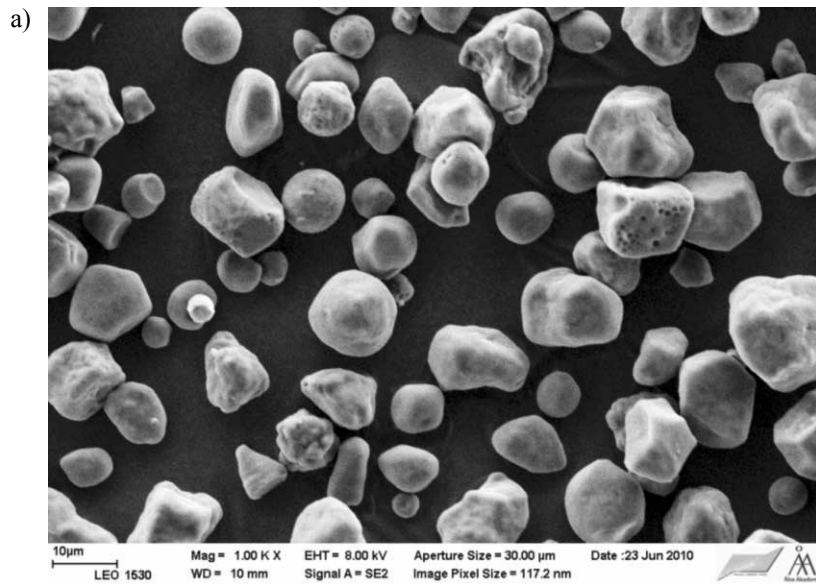


Figure 3.30. a) Unmodified, b) oxidized, high containing amylopectin corn starch (semibatch, pH = 8.4, T = 55 °C), zoom 1000x.

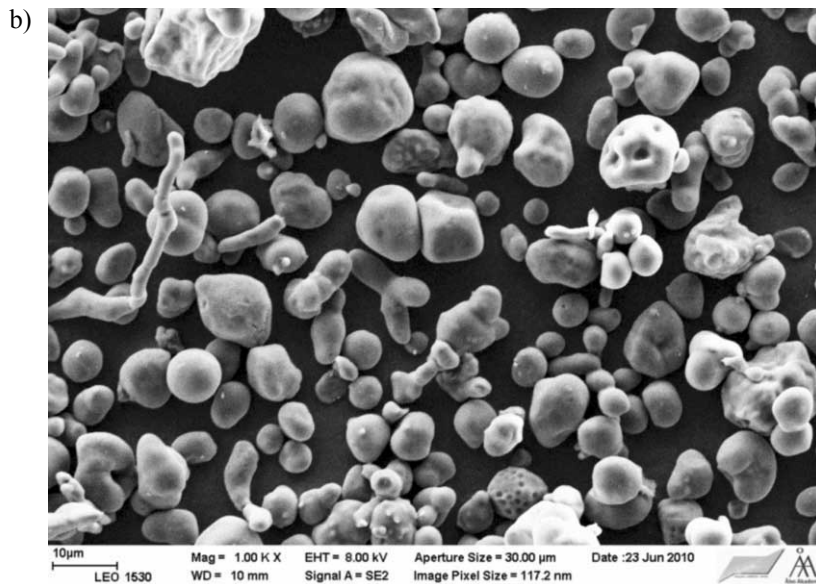
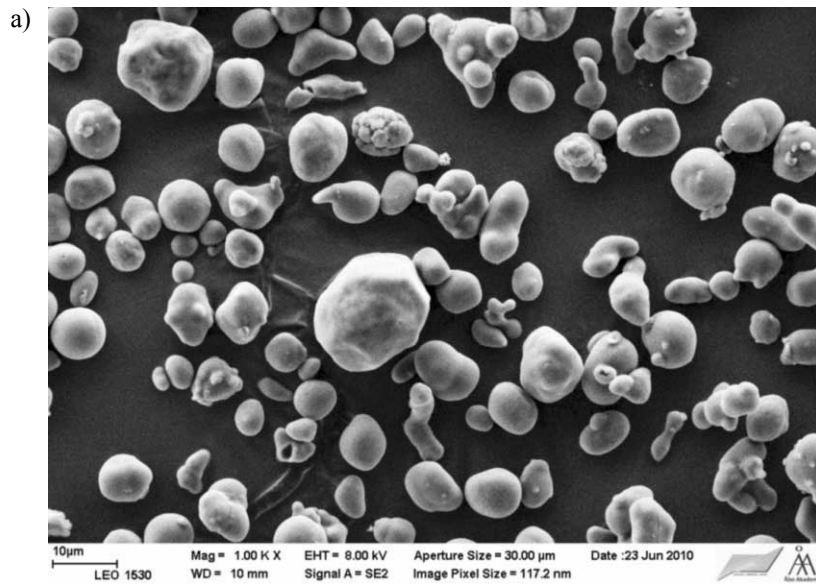


Figure 3.31. a) Unmodified, and b) oxidized, high containing amylose corn starch (batch, pH = 8.4, T= 55 °C), zoom 1000x.

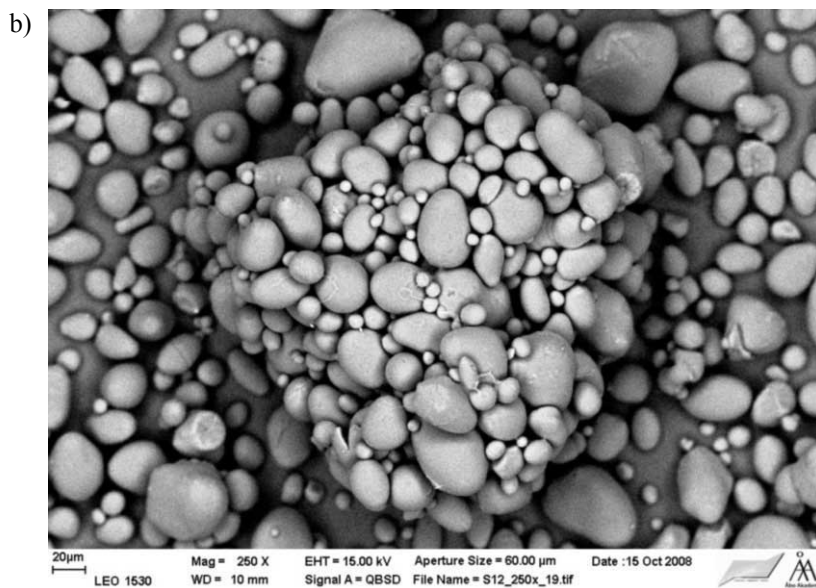
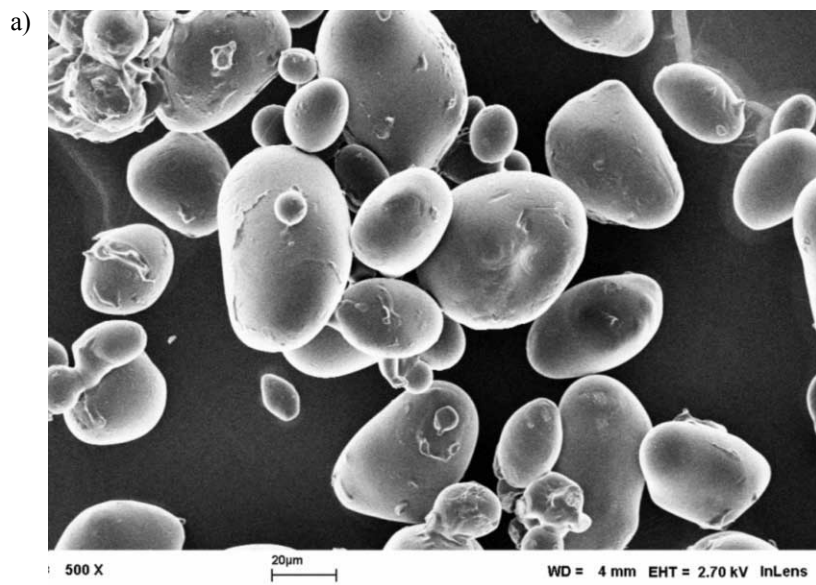


Figure 3.32. Potato starch oxidized with FePcS, at 55 °C, semibatch and **a)** pH = 7, 500x, and **b)** pH = 8.4, 250x.

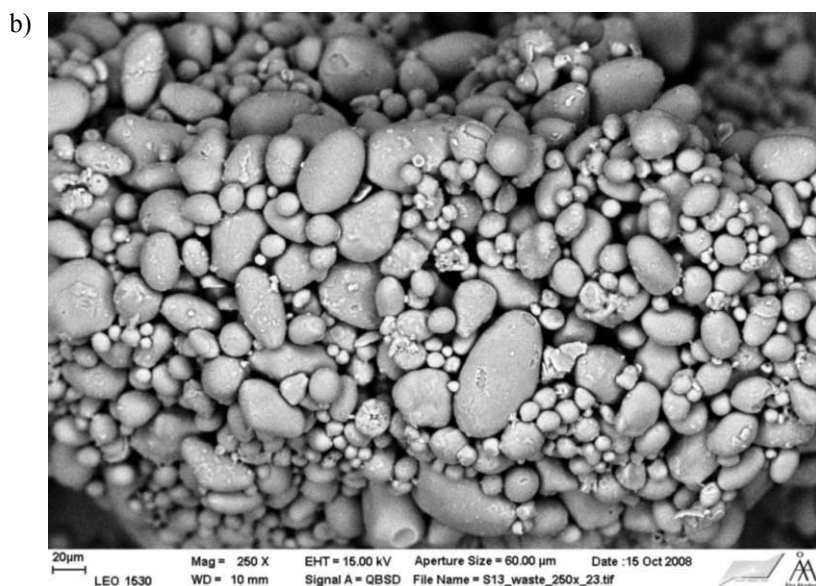
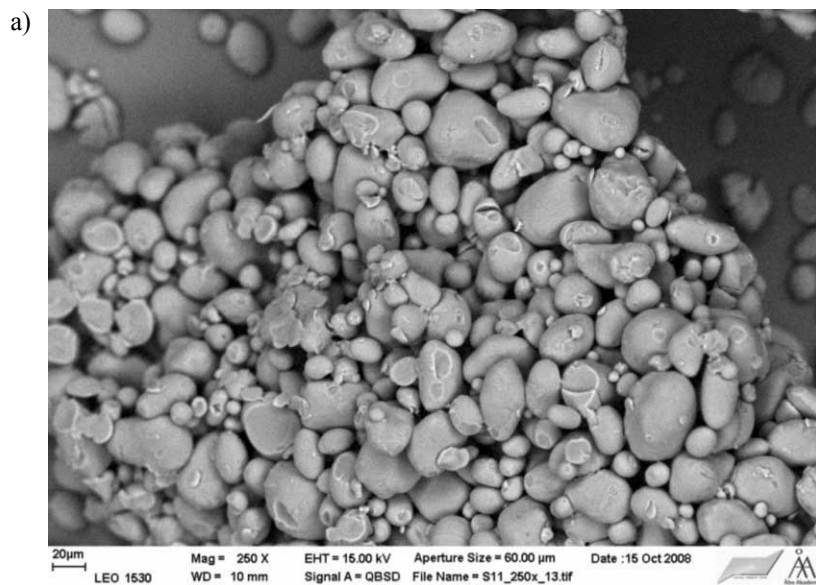


Figure 3.33. a) Potato starch oxidized with FePcS, at 55 °C, semibatch and pH 10, and b) potato starch oxidized by iron sulphate (FeSO_4) at 55 °C, semibatch and pH 2-4.

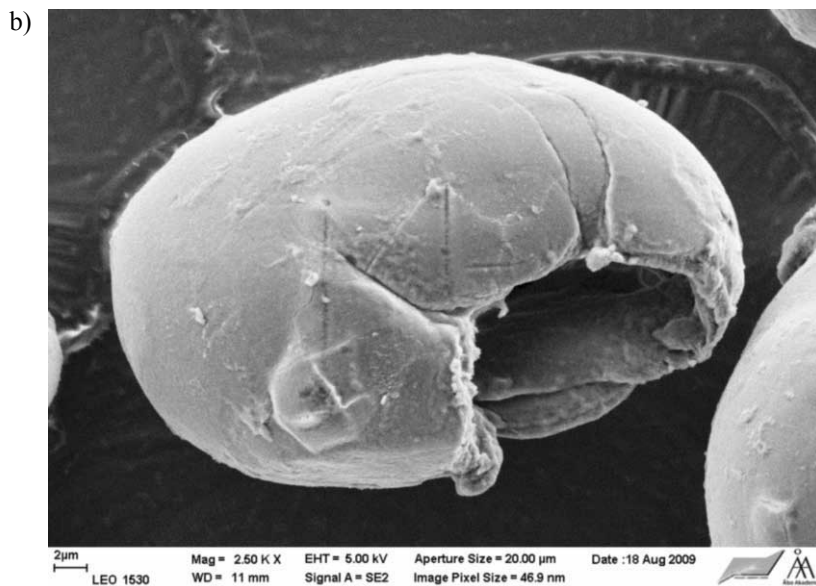
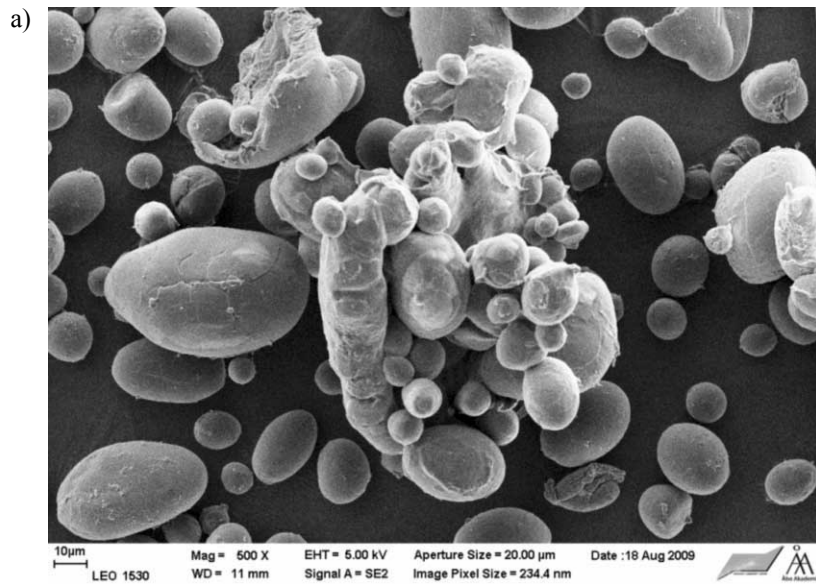


Figure 3.34. Potato starch oxidized by H_2O_2 and FePcS in batch mode, 52 °C and pH 7.5 a) 500x and b) 2500x

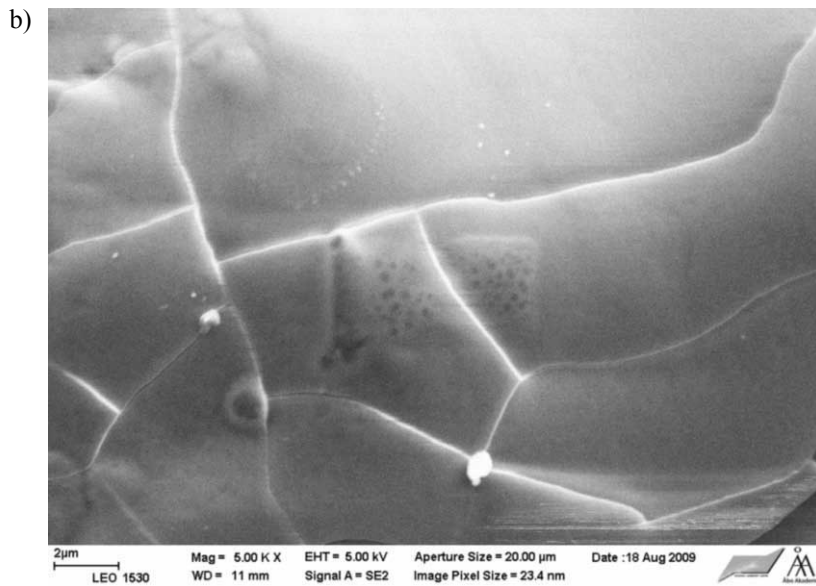
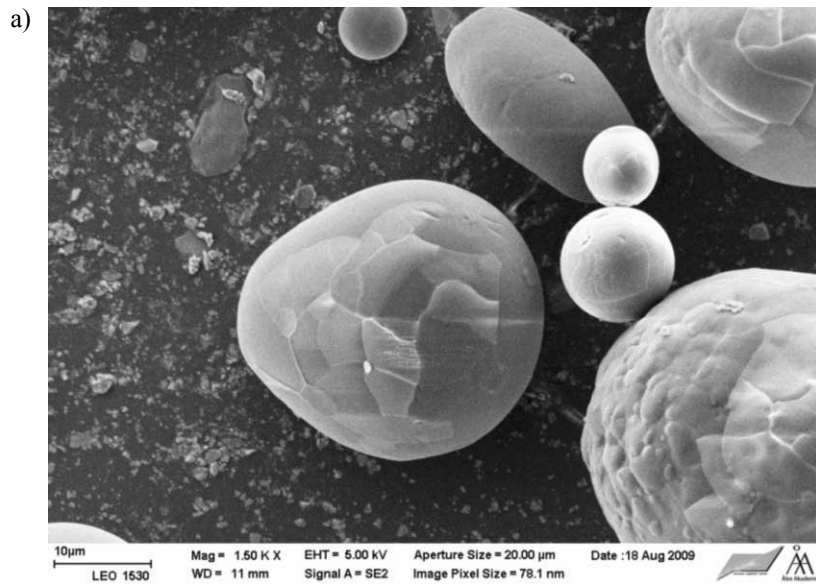


Figure 3.35. unmodified potato starch only treated with ultrasound for 24 h a) 1500x, b) 5000x.

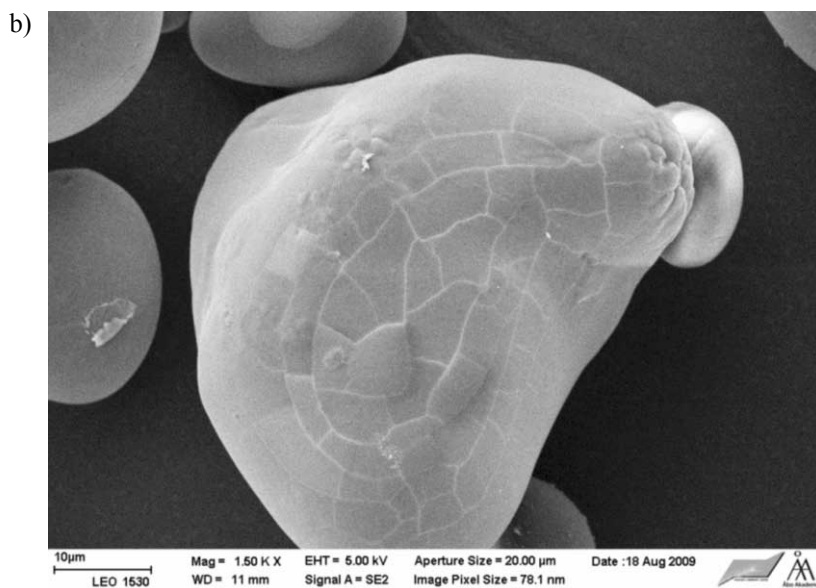
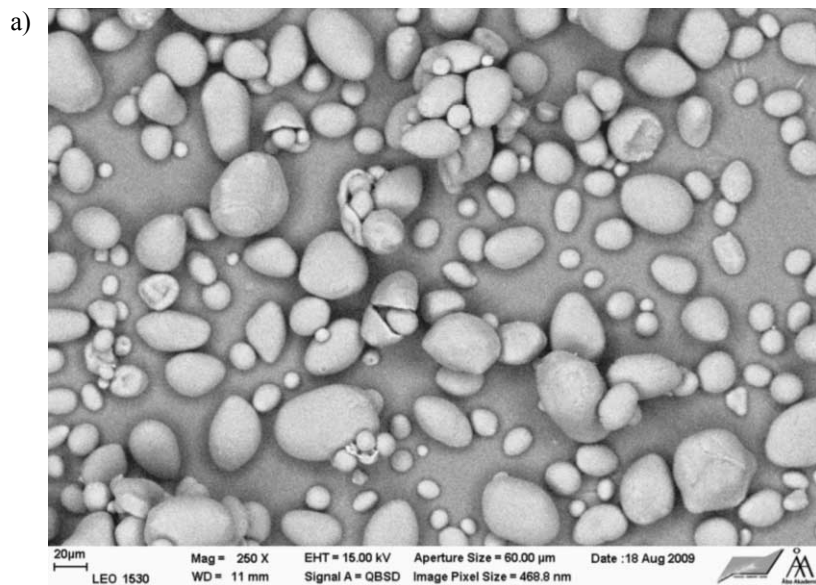


Figure 3.36. Ultrasound pretreated potato starch oxidized by H_2O_2 and FePcS at pH = 8.4, 55 °C in batch mode **a)** 250x, **b)** 1500x.

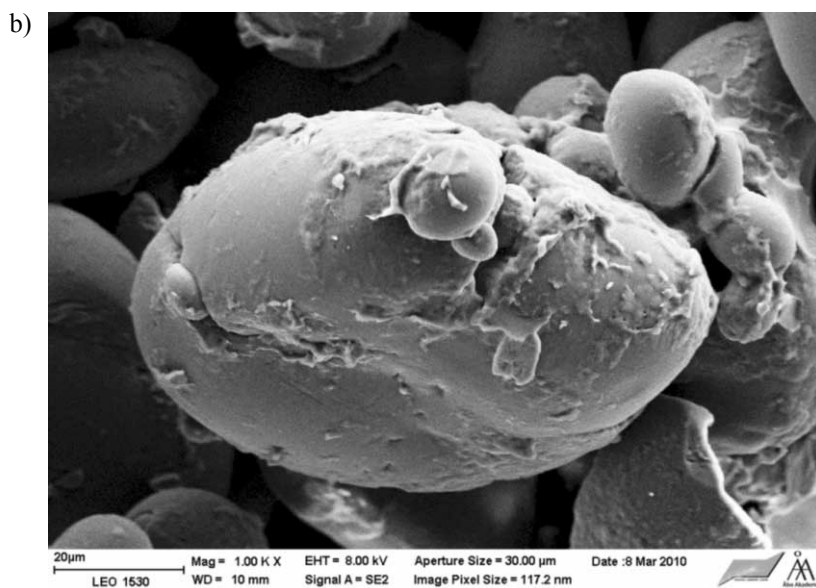
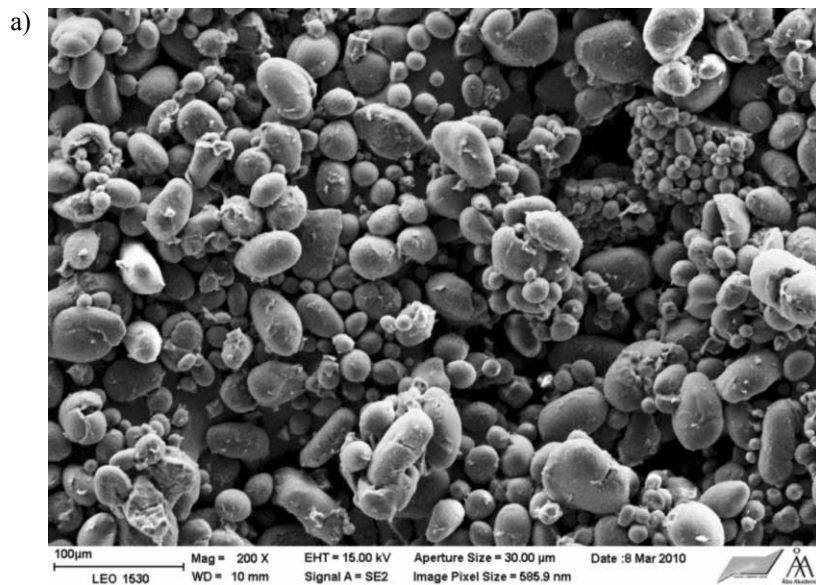


Figure 3.37. Potato starch after simultaneous batch oxidation with FePcS and ultrasonification at pH = 8.4 **a)** 50x, **b)** 1000x.

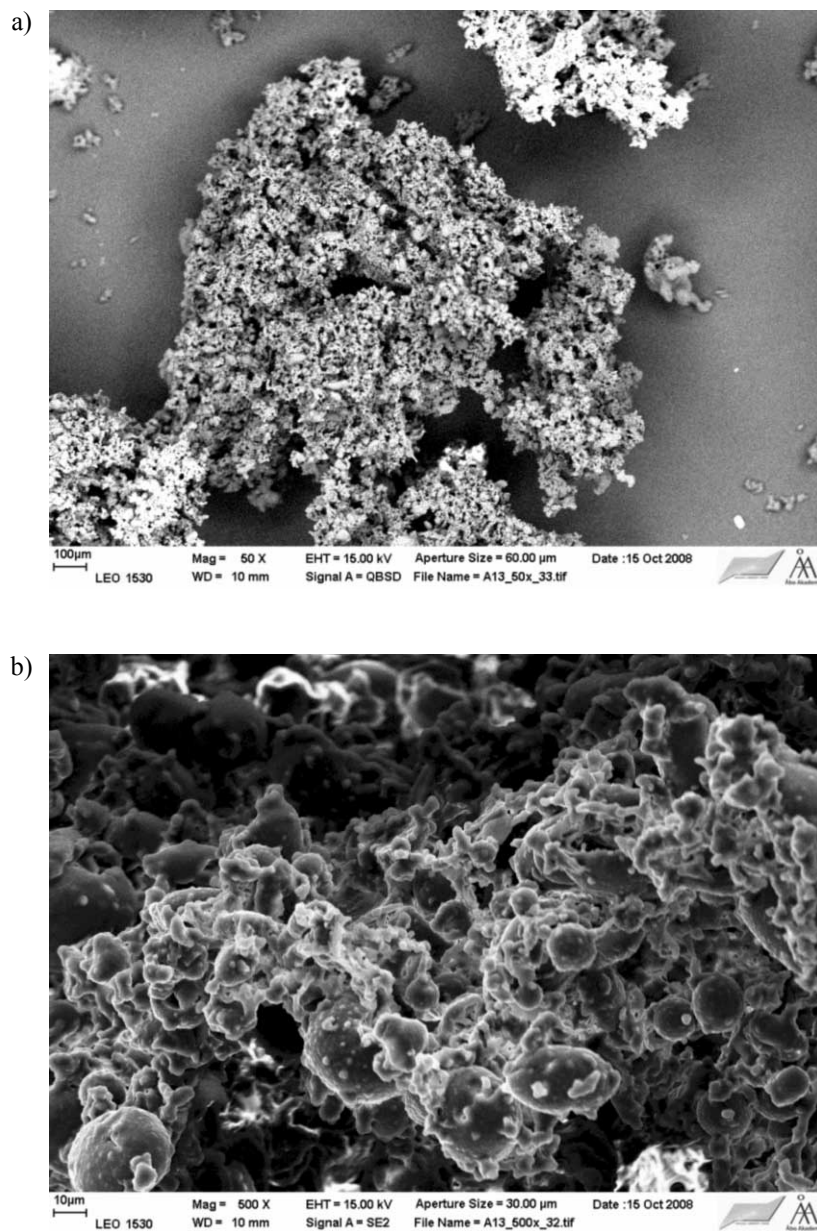


Figure 3.38. Batch oxidation with FePcS catalyst, performed in a bottle with starting pH = 8.6 and final pH = 2.25 (Table 1, art1, entry 13), **a)** 50 x, **b)** 500x.

3.15 Product coloration

It was noticed that after oxidation reaction of the starch, the solid particles were prone to coloration due to the catalyst used. The most coloration was found when using iron sulphate as catalyst, then leaving the starch a light brown color which stayed even after a rigorous washing treatment (figure 3.39, left). Also the FePcS catalyst left a paly greenish color to the solid starch at higher pH values (10), whereas at pH 8.4 the final product was colorless, as the final reaction solution as well lost the blue color.



Figure 3.39. Potato starch oxidized by the catalyst FeSO_4 (left), potato starch oxidized by the catalyst FePcS at pH = 10 (center), and potato starch oxidized by FePcS at pH = 8.4 (right).



Figure 3.40. The color change of the reaction media during an semibatch oxidation experiment when using H_2O_2 and FePcS catalyst and $\text{pH} = 8.4$. From left to right: reaction time 10 min, 180 min and 420 min.

4. CONCLUSIONS

A new, environmentally friendly method for homogeneously catalyzed oxidation of starch by hydrogen peroxide has been developed and kinetic data have been recorded from semibatch experiments in order to receive information regarding the carboxyl and carbonyl group formation, as well as the yield of oxidized starch. Numerous batch experiments were carried out to receive important data regarding the decomposition of H_2O_2 . The effect of catalyst addition policy on the carboxyl group formation has been studied, as well.

Batch experiments were performed at different pH to reveal the kinetics of the partial starch oxidation with FePcS as a catalyst and H_2O_2 as an oxidant. A faster oxidation reaction and also more significant loss of solid starch due to depolymerization was observed at higher pH. The degree of carboxyl groups substitution in the batch mode was maximally $DS_{COOH} = 0.73$ at 52 °C, whereas it was about $DS_{COOH} = 1.62$ in the semi-batch mode as the catalyst was continuously fed into the system (Table 3.3). This result can be explained by the fact that H_2O_2 decomposition was faster in the batch experiments due to the high concentration. By adding the catalyst continuously in to the reactor, a higher DS was achieved with the same amount of catalyst compared to the batch mode. By pre-treating the starch with ultrasound, higher surface area of starch was obtained due to the formation of pores or cavities, thus leading to a higher degree of substitution (60% higher) than by using the native starch only. Preliminary it can be said that ultrasound can be a promising technique to improve the starch oxidation process.

Addition of the hydrogen peroxide semibatch-wise resulted in higher degrees of substitution, compared to the batch mode experiments. Adding the catalyst to the reaction solution in semibatch mode instead of the hydrogen peroxide improved the DS yield even further. The semibatch results had, however, a rather complex kinetic behavior and, therefore, batch mode experiments were performed to investigate the reaction mechanisms in more detail. The influence of the catalyst concentration had a larger impact on the H_2O_2 decomposition, whereas the solid-to-liquid ratio did not influence the H_2O_2 decomposition remarkably. A mathematical model for the decomposition of hydrogen peroxide was developed. The use of ultrasound for the pretreatment of starch particles improved the reactivity of starch, but using ultrasound during the oxidation did not improve the DS significantly. From SEM analysis, a clear deterioration of the granule surfaces was identified, which explains the positive effect of ultrasound.

NOTATION

c	concentration
E_a	activation energy
K	equilibrium constant
k	rate constant
R	general gas constant
R^2	degree of explanation
r	reaction rate
T	temperature
t_r	reaction time
y	dependent variable in regression
α	merged rate parameter
δ	reaction order
θ	objective function in regression
[]	concentration

Subscripts and superscripts

ave	average temperature
cat	catalytic
I_1	complex
nonc	non-catalytic
X	catalyst
0	reference or initial value

Abbreviations

AGU	anhydroglucose unit
BET	Brunauer-Emmet-Teller
MS	mass spectrometry
SEM	Scanning electron microscopy
Q-TOF	Quadrupole time of flight mass spectrometer

REFERENCES

- 1 Starch: Chemistry and technology, third edition 2009 edited by BeMiller, Whistler.
- 2 Ir. J. J. M. Swinkels, Composition and properties of commercial native starches. *Starch/Stärke*, 37 (1985) 1–5.
- 3 Evaluation of common agricultural policy measures applied to the starch sector, final report - AGROSYNERGIE – November 2010.
- 4 <http://www.starch.dk/ist/app/paper.asp> (11.01.2013)
- 5 R. N. Tharanathan, Starch - value addition by modification. *Critical reviews in food science and nutrition*, 45 (2005). 371–384.
- 6 K. Sangseethong, N. Termvejsayanon, K. Sriroth, Characterization of physicochemical properties of hypochlorite and peroxide-oxidized cassava starches. *Carbohydrate Polymers*, 82 (2010) 446–453.
- 7 S. Komulainen, C. Verlackt, J. Pursiainen, M. Lajunen, Oxidation and degradation of native wheat starch by acidic bromate in water at room temperature. *Carbohydrate Polymers* (2012), in press.
- 8 P. Tolvanen, P. Mäki-Arvela, A.B. Sorokin, T. Salmi, D.Yu. Murzin, Kinetics of starch oxidation using hydrogen peroxide as an environmentally friendly oxidant and an iron complex as a catalyst. *Chemical Engineering Journal* 154(1-3) (2009) 52-59.
- 9 P. Tolvanen, P. Mäki-Arvela, A. B. Sorokin, S. Leveneur, T. Salmi, D. Yu. Murzin, Batch and semi-batch partial oxidation of starch by hydrogen peroxide in the presence of iron tetrasulfophthalocyanine catalyst: the effect of ultrasound and catalyst addition policy. *Industrial & Engineering Chemistry Research*, 50(2) (2011) 749-757.

- 10 D. Kuakpetoon, Y.-J. Wang, Locations of hypochlorite oxidation in corn starches varying in amylose content. *Carbohydrate Research* 343 (2008) 90–100.
- 11 K. Sangseethong, N. Termvejsayanon, K. Sriroth, Characterization of physicochemical properties of hypochlorite and peroxide-oxidized cassava starches. *Carbohydrate Polymers* 82 (2010) 446–453.
- 12 H. W. Hsein-Chih, A. Sarko, The double-helical molecular structure of crystalline b-amylose. *Biopolymers*, 61 (1978) 7-40.
- 13 R.E. Wing , J.L. Willett, Water soluble oxidized starches by peroxide reactive extrusion. *Industrial Crops and Products*, 7 (1997) 45-52.
- 14 BASF press release: www.basf.com/group/pressrelease/P-10-179 (20.10.2012)
- 15 Nigel Williams, One new potato. *Current Biology*, 20 (2010) R301.
- 16 P. Tomasik, C. H. Schilling. Chemical modification of starch. *Advances in Carbohydrate Chemistry and Biochemistry*, 59 (2004) 175-403.
- 17 P. Forssell, A. Hamunen, A. Antio, T. Surotti, K. Poutanen, Hypochlorite oxidation of barley and potato starches. *Starch/Stärke*, 47 (1995) 371–377.
- 18 A. B. Sorokin, S. L. Kachkarova-Sorokina, C. Donzé, C. Pinel, P. Gallezot, From native starch to hydrophilic and hydrophobic products: a catalytic approach. *Topics in Catalysis*, 27 (2004) 67-76.
- 19 M. Floor, K. M. Schenk, A. P. G. Kieboom, H. van Bekkum, Oxidation of maltodextrins and starch by the system tungstate-hydrogen peroxide. *Starch/Stärke*, 41 (1989) 303-309.

- 20 D. Kuakpetoon, Y-J. Wang, Locations of hypochlorite oxidation in corn starches varying in amylose content. *Carbohydrate Research*, 343 (2008) 90-100.
- 21 H. S. Isbell, H.L. Frush, Mechanisms for hydroperoxide degradation of disaccharides and related compounds. *Carbohydrate Research*, 161 (1987) 181-193.
- 22 S. M. Butrim, T. D. Bil'dyukevich, T. L. Yurkshtovich. Kinetics of starch oxidation in the system nitrogen (IV) oxide-tetrachloromethane. *Russian Journal of Applied Chemistry*, 74 (2001) 2106-2110.
- 23 P. Mischnick-Lübbecke, W. A. König, Bestimmung der Substitutionsmuster von chemisch modifizierten Stärken, *Starch/Stärke*, 39 (1987) 425-431.
- 24 P. Parovuori, A. Hamunen, P. Forssell, K. Autio, K. Poutanen, Oxidation of potato starch by hydrogen peroxide. *Starch/Stärke*, 47 (1995) 19-23.
- 25 S. Veelaert D. de Wit, H. Tournois, An improved model for the periodate oxidation of starch. *Polymer* 35 (1994) 5091-5097.
- 26 W. Armstrong, Relative rate constants for reactions of hydroxyl radicals from the reactions of iron (II) or titanium (III) with hydrogen peroxide. *Canadian Journal of Chemistry* 47 (1969) 3737-3744.
- 27 A. Sorokin, B. Meunier, Oxidation of polycyclic aromatic hydrocarbons catalyzed by iron tetrasulfophthalocyanine FePcS: inverse isotope effects and oxygen labeling studies. *European Journal of Inorganic Chemistry*, 9 (1998) 1269-1281.
- 28 J. H Weber, D. H. Busch, Complexes derived from strong field Ligands. XIX. Magnetic properties of transition metal derivatives of 4,4',4'',4'''-tetrasulfophthalocyanine. *Inorganic Chemistry*, 4 (1965) 469.

- 29 A. Hadasch, A. Sorokin, A. Rabion, L. Fraisse, B. Meunier, Oxidation of 2,4,6-trichlorophenol (TCP) catalyzed by iron tetrasulfophthalocyanine (FePcS) supported on a cationic ion-exchange resin. *Bulletin de la Société chimique de France*, 134 (1997) 1025-1032.
- 30 R. J. Smith, Characterization and analysis of starches. *Starch: Chemistry and Technology*, Eds. R.I. Whistler and E.F. Paschall, Volume II, Academic Press, Inc., New York 1967, pp. 620-625.
- 31 H. Grénman, E. Murzina, M. Rönnholm, K. Eränen, J.-P. Mikkola, M. Lahtinen, T. Salmi, D. Yu. Murzin, Enhancement of solid dissolution by ultrasound. *Chemical Engineering and Processing*, 46 (2007) 862–869.
- 32 T. Salmi, H. Grénman, H. Bernas, J. Wärnä, D. Yu. Murzin, Mechanistic modelling of kinetics and mass transfer for a solid–liquid system: leaching of zinc with ferric iron. *Chemical Engineering Science*, 65 (2010) 4460–4471.
- 33 S. Pietrzyk, T. Fortuna, Ł. Raś, The influence of pH and Fe (II) ions on physicochemical properties of oxidized potato starch. *Electronic Journal of Polish Agricultural Universities*, 10(4) (2007) 16.
- 34 N. d’Alessandro, L. Tonucci, M. Bressan, L. K. Dragani, A. Morvillo, Rapid and selective oxidation of metallosulfophthalocyanines prior to their usefulness as precatalysts in oxidation reactions. *European Journal of Inorganic Chemistry*, 9 (2003) 1807-1814.
- 35 J. H. M. Hovenkamp-Hermelink, J. N. De Vries, P. Adamse, E. Jacobsen, B. Witholt and W. J. Feenstra, Rapid estimation of the amylose/amylopectin ratio in small amounts of tuber and leaf tissue of the potato. *Potato Research*, 31 (1988) 241-246.

- 36 H. Haario, MODEST Users guide, Profmath Oy, Helsinki 2007.
- 37 G. Tachiev, J. A. Roth, A. R. Bowers, Kinetics of hydrogen peroxide decomposition with complexed and “free” iron catalysts. *International Journal of Chemical Kinetics*, 32 (1999) 24-35.
- 38 N. N. Mahamuni, P. R. Gogate, A. B. Pandit, Selective synthesis of sulfoxides from sulfides using ultrasound. *Ultrasonics Sonochemistry*, 14 (2) (2007) 135-142.
- 39 D. Yu. Murzin, T. Salmi, *Catalytic kinetics*, Elsevier 2005.
- 40 Aytunga Arik Kibar, Gelatinization of Waxy, Normal and High Amylose Corn Starches. *The Journal of Food*, 35 (2009) 1-8.

LIST OF PUBLICATIONS

P. Tolvanen, P. Mäki-Arvela, A. B. Sorokin, T. Salmi, D.Yu. Murzin, Oxidation of starch by H_2O_2 in the presence of iron tetrasulfophthalocyanine catalyst: the effect of catalyst concentration and solid-to-liquid ratio and origin of starch, *submitted*, (2013).

P. Tolvanen, P. Mäki-Arvela, A. B. Sorokin, S. Leveneur, T. Salmi, D. Yu. Murzin, Batch and semi-batch partial oxidation of starch by hydrogen peroxide in the presence of iron tetrasulfophthalocyanine catalyst: the effect of ultrasound and catalyst addition policy, *Industrial & Engineering Chemistry Research*, 50 (2011) 749–757.

P. Tolvanen, P. Mäki-Arvela, A. B. Sorokin, T. Salmi, D. Yu. Murzin, Kinetics of starch oxidation using hydrogen peroxide as an environmentally friendly oxidant and an iron complex as a catalyst, *Chemical Engineering Journal*, 154 (2009) 52-59.

P. Tolvanen, P. Mäki-Arvela, N. Kumar, K. Eränen, J. Wärnä, B. Holmbom, T. Salmi, D. Yu. Murzin, Thermal Polymerisation and Autoxidation of Technical Grade Linoleic Acid, *Journal of the American Oil Chemists' Society*, 85(6) (2008) 567-572.

P. Tolvanen, P. Mäki-Arvela, N. Kumar, K. Eränen, R. Sjöholm, J. Hemming, B. Holmbom, T. Salmi, D. Yu. Murzin, Thermal and catalytic oligomerisation of fatty acids, *Applied Catalysis A: General*, 330 (2007) 1-11.

P. Mäki-Arvela, P. Tolvanen, N. Kumar, K. Eränen, R. Sjöholm, B. Holmbom, D. Yu. Murzin, T. Salmi, Catalytic transformation of fatty acids to biodiesel and fine chemicals — Suppression of side reactions, submitted to 3rd International Conference on Green and Sustainable Chemistry 1-5 July 2007, Delft.

Oral presentations

Oral presentation, International Conference Catalysis For Renewable Sources: Fuel, Energy, Chemicals, June 27-02.07 2010, St. Petersburg, Russia. The Effect Of Ultrasound On Catalytic Starch Oxidation By Hydrogen Peroxide, P. Tolvanen, P. Mäki-Arvela, D. Yu. Murzin, T. Salmi.

Oral presentation, 8th World Congress of Chemical Engineering (WCCE8), August 23-27 2009, Montréal, “Environmentally friendly catalytic starch oxidation by hydrogen peroxide”. P. Tolvanen, P. Mäki-Arvela, A. B. Sorokin, T. Salmi, D. Yu. Murzin.

Oral presentation, Chemreactor-18, Malta 29.09 2008, “Kinetics of starch oxidation using hydrogen peroxide as an environmentally friendly oxidant and an iron complex as a catalyst”, P. Tolvanen, P. Mäki-Arvela, A. B. Sorokin, T. Salmi, D. Yu. Murzin.

Poster presentations

15th Nordic symposium on catalysis, 2012, Partial starch oxidation by hydrogen peroxide and a metal complex as catalyst.

ECCE Berlin, 2011, Parameters in batch-wise starch oxidation.

CHISA Prague, 2010, Kinetics and modeling of catalytic starch oxidation by H₂O₂.

PCC annual meeting, 2008, Kinetic study of catalytic starch oxidation using hydrogen peroxide.

Reports

P. Tolvanen, "Kinetic study of organic reactions", Laboratory of Industrial Chemistry, Process Chemistry Centre, Department of Chemical Engineering, Å.A., 2012.

P. Tolvanen, "Esterification of stearyl alcohol with carboxylic acids", Laboratory of Industrial Chemistry, Process Chemistry Centre, Department of Chemical Engineering, Faculty of Technology, Å.A., 2007.

Translation of master thesis to Finnish, "Rasvahapporeaktion terminen ja katalyyttinen kinetiikka", 2006.

P. Tolvanen, Master Thesis in Swedish "Termisk och katalytisk kinetik av en fettsyrareaktion", Processkemiska centret, Kemisk-tekniska fakulteten, Åbo Akademi, 2006.



9 789521 228346 >